UNIVERSIDADE DA BEIRA INTERIOR
Engenharia

Pressure and Deformation Measurement with Piezoresistive Sensors

José Henrique Fernandes Pimentel

Dissertação para obtenção do Grau de Mestre em
Engenharia Eletrotécnica e de Computadores
(2º ciclo de estudos)

Orientador: Prof. Doutor António Espírito Santo
Coorientador: Prof. Doutor Senentxu Lanceros

Covilhã, junho de 2017

Acknowledgments

I would like to express my special thanks and gratitude to my supervisor Professor António Espírito Santo for encouraging me in the continuation of my studies in Electrical and Computers Engineering and for support me when I wanted to make my Erasmus internship. For all the motivation that he gave me during the more stressing times, thank you.

A special thanks to my co-supervisor Professor Senentxu Lanceros, who gave the opportunity to make part of BCMaterials research team, in Spain, for an internship. For all the activities in Bilbao, for the motivation during the internship and for teaching me about Basque country, thank you.

To Pedro Costa from University of Minho, who helped me during all this work, shared his knowledge during my internship and was always available for everything I needed. His friendship during my stay in Bilbao was very important for me. Not only for the work and the patience he spent with me but also for the adventures that we had in Bilbao, thank you very much Pedro.

I would like to thank the BCMaterials team that was always amazing with me during my stay. Fantastic people, fantastic place, excellent team. Thank you for the opportunity.

For my friends from university and from the laboratory. For all the good moments that I will always remember, thank you.

To Carolina that always accompanied me and helped me, especially in the most difficult moments. For all the patience during this last year and for the help during the review of this work, thank you.

Lastly but must important of all, to my family, in special to my parents who are the basis of everything I have. For all the opportunities that they gave me on my life, I want to say thank you and I love you mum and dad.

Resumo

Esta dissertação vem mostrar o processo completo para o desenvolvimento de um sensor capaz de medir deformações de superfícies. O trabalho passa assim pelos processos de produção e montagem dos transdutores, pelos circuitos eletrónicos desenhados para fazer as leituras do transdutor e finalmente pelos algoritmos utilizados para transformar o sinal do sensor numa informação que pode ser interpretada por humanos ou por outras máquinas.

Desta forma, o trabalho inicia-se por um estudo dos métodos de produção e montagem dos transdutores. No final optou-se pela técnica de *screen printing* para produzir os transdutores e os elétrodos. Quanto ao método de montagem, optou-se por fazer uma sobreposição das camadas impressas.

Após termos o transdutor impresso conseguimos testá-lo e assim obter informações como a variação da resistência. Estes são parâmetros muito importantes para o dimensionamento da cadeia de medida, que foi o segundo passo deste trabalho. Foi desenhada uma cadeia de medida capaz de fazer a leitura de diferentes sensores ao mesmo tempo. Este circuito é também capaz de se adaptar a diferentes sensores automaticamente.

Como os sensores testados neste projeto apresentaram histerese, para contornar esta situação, um modelo de aproximação utilizado com materiais magnéticos foi adaptado para os sensores piezoresistivos.

O trabalho cumpre o objetivo proposto no início deste projeto que era construir um sistema completo de aquisição de dados de um sensor piezoresistivo impresso. No final foi introduzido a adaptação do algoritmo que abre portas para futuros trabalhos.

Palavras Chave

Sensores piezoresistivos, sensores impressos, aquisição de dados, modelo de Preisach

Resumo Alargado

Este trabalho dá continuidade aos estudos já feitos em sensores piezoresistivos nos nossos laboratórios, no entanto acaba por tocar nesta matéria de um ponto de vista diferente dos anteriores. Em vez de nos focarmos no material ou na componente eletrónica, fez-se uma abordagem mais do ponto de vista do teste de como ambas as componentes têm de funcionar entre si.

O objetivo final do trabalho é conseguir obter o sinal de um sensor piezoresistivo construído por nós e quantifica-lo. Foi utilizado um transdutor constituído por um compósito de polímero com nanotubos de carbono. O transdutor, devido aos seus constituintes, tem uma grande capacidade de deformação o que o torna bom para aplicações que exijam estas caraterísticas, como por exemplo a medição da deformação durante o movimento de articulações ósseas.

Um segundo transdutor foi também utilizado. Desta vez utilizou-se um transdutor que já está no mercado. Este transdutor serviu para comparação de resultados em relação ao transdutor que foi construído em laboratório.

No que diz respeito à montagem do transdutor, optou-se pela sobreposição de camadas devido às condições que tínhamos, no entanto, são demonstrados outros métodos, como a deposição de camadas que é semelhante ao método utilizado, mas com uma diferença. As camadas são depositadas diretamente umas em cima das outras.

Após a conclusão de produção e montagem do transdutor passou-se para a construção do sistema de aquisição de dados. Sendo assim, para controlar o sistema de aquisição utilizou-se o microcontrolador LPC1768 integrado na plataforma mbed. Com os componentes eletrónicos utilizados foi construída uma cadeia de aquisição que é capaz de se adaptar a sensores com valores de resistência iniciais diferentes, o que tornou esta plataforma altamente adaptável e útil para testes em diferentes tipos de sensores. Para conseguir esta adaptabilidade foram utilizados reóstatos digitais que, através de *software* conseguem colocar-se na melhor posição, dentro dos seus limites, para darem os resultados com o máximo de sensibilidade possível.

Os dados após serem adquiridos pelo microcontrolador serão enviados para um computador que vai mostrar os mesmos numa forma gráfica. Estes dados são enviados por serial, através da porta USB, ou por ligação sem fios, utilizando o módulo *wi-fi* RN-171.

Como os transdutores testados apresentam histerese, estudaram-se modelos para fazer aproximações mais exatas. Para este projeto foi utilizado o modelo de *Preisach*. Este modelo é utilizado para contornar a histerese caraterística dos materiais magnéticos, no entanto, foi adaptado o código em *Matlab* para funcionar com estes sensores. No final conseguiu-se ter uma aproximação teórica dos valores que poderão ser obtidos.

Abstract

This dissertation shows us the processes to develop a sensor capable of measuring deformations of surfaces. The work englobes the processes of production and assemblage of the transducers, the electronics boards to read the signals from the transducers and, finally, the development of algorithms used to transform the signal of the sensor in readable information either for humans and other computers.

The work starts with the study of the production and assemblage methods of the transducers. In this part, we used the screen printing technique to print the different layers of the transducer.

After obtaining the printed transducer, we tested it, measuring only the main characteristics, as the variation of resistance with pressure. This gave us important information to proceed with the dimensioning of the measurement chain.

The second part of this project, was focused in the design of the measurement chain. For this work, we projected a device that can adapt automatically to different values of sensors' resistance.

Because the transducers tested in this project have a hysteretic behavior, a mathematical model used to model the magnetic hysteresis was adapted to be used with piezoresistive sensors.

This work meets the initial goal which was building a complete data acquisition system for a printed piezoresistive sensor. The proposed mathematical algorithm to model the resistance of piezoresistive sensors opens doors for future projects.

Keywords

Piezoresistive sensors, printed sensors, data acquisition, Preisach model

Table of Contents

List of Figures

List of Tables

Glossary

PS	Piezoresistive Sensor
SCLK	Serial Clock
SPI	Serial Peripheral Interface
CS	Chip Select
MISO	Master In Slave Out
MOSI	Master Out Slave In
MWCNT	Multi Walled Carbon Nanotubes
CPME	Cyclopentyl Methyl Ether
ADC	Analog to Digital Converter
CNT	Carbon Nanotubes
SEBS	Styrene Ethylene Butylene Styrene
USB	Universal Serial Bus
PC	Personal Computer
MCU	Micro Controller Unit
PCB	Printed Circuit Board
FDA	Food and Drug Administration
GUI	Graphic User Interface

1. Introduction

1.1 Motivation

Living beings have their own sensing systems. While this dissertation is being written or while it's being read there are millions of sensors informing our brain about everything around and inside us. Although we have the necessary sensors to live, there are a plenty of signals we can't sense, for example, we cannot quantify the temperature of a room or the weight of an object. In the past, this was not a problem, but due to mankind evolution and with our ambition to measure and control everything, instruments with the capability to measure things for us has become fundamental. Nowadays, in a developed world, it is unthinkable to live without sensors. They allow us to measure parameters that before we couldn't.

The beauty of the sensors' world is that we can measure almost everything we want and transform it into an electric signal that can be translated to control systems in the engineering, health or environmental fields.

1.2 Main Goal

The main goal of this project is to develop a prototype of a sensing device, that can be used in biomedical applications. This device will be based on the newest smart materials merged with electronics and algorithms. The outcome of the development work performed in this project, will be a complete data acquisition system, capable of making the right translation of the pressure applied in a surface, and present the information correctly to the user.

1.3 Framework

Mankind has developed sensors that can go from measuring body temperature, to measuring the electrical potentials in our heart to help people with an irregular heartbeat. Nowadays, sensors are used in areas as industry, agriculture, transports, domestic devices, military, biomedical devices, among others. Almost every machine has some kind of sensing device inside. With "Smart World" advent, sensors are becoming more present and important in our society.

The relation between new technologies and biological systems is becoming more and more closed. We, humans, want to measure everything, save every single data and access it from wherever we are, and we don't want to wait hours or days to have our results, we want to check everything in real time. In some situations, this is already a reality in our world. We can use smart watches that measure the heart rate while we are running, sleeping or working, or we can check our breath rate to detect sleep apnea, for instance. The evolution of the technology made all this possible and affordable to everyone.

Sensors' world includes multiple areas depending on what we want to measure. Currently an area that is receiving increasing attention is the biomedical field. This interest brings to the science community new challenges, because it's not easy to have a device or a material that makes what we want and, at the same time, is compatible with biological systems. Researchers are taking advantage of new compounds to produce sensors which have similar behaviours with the usual sensors and that are biocompatible, so they can be used in biologic organisms.

Sensors alone are not enough to get signals from the environment. It's like in our body, only with our eyes, we could not see, it's necessary to take information to our brain, to be processed, and give us what we call the vision. So, an entire measurement chain needs to be constructed if we want to have a small sensor measuring the temperature somewhere and send this information by a wireless connection to a decision center.

Technology usually is associated with the use of energy. This presents another issue to the engineers these days because there are two divergent situations. We want improved devices that can measure parameters with increased precision. To difficult more the situation, sometimes we want to make this in remote environments, with no access to the electrical power grid. To achieve this goals, we need to use devices as efficient as possible, in order to get a sustainable operation from the energy point of view. To solve this problem, we make use of low power devices that need low amounts of energy to work. This is not only possible because the devices are designed to waste less energy but also because we can program them to operate in an efficient way.

1.4 Applications

Piezoresistive sensors (PS) are still rather unknown when compared with sensors that measure temperature or glucose, for example. One of the first questions raised when talking about PSs is why we need them and what's their function. However, there are many areas of application for PSs. Some of them are biomedical, industry or household.

In household applications, PSs can be applied from washing machines, to smartphone, sensitive carpets, anti-rob systems and prevision of natural catastrophes, as earthquakes. Other example is a recent study that shows a prototype for a sensing glove that could be used with exoskeletons to help people during household works [1].

In industry, for instance, in automotive industry, PSs are used in engine optimization and safety enhancement. In the first case, PSs are used to control the intake air pressure and barometric air pressure for the engine, allowing optimal engine operation. In safety enhancement, we have multiple areas where the use of PSs is welcomed. For example, to check the tires' pressure or control the deployment of the airbags for different kinds of impacts.

Finally, in the biomedical field, many applications for PSs can be found. We can measure the air pressure in our lungs, the heartbeat strength, the movement of the body or even use them to control exoskeleton models.

As we can see, PSs have a large field of applications in different areas. There are many other applications for PSs. However, some of these applications require specifications from the sensors that don't exist in the natural form, so they should be developed. For example, if we want a PS that is, simultaneously able to support high levels of deformation and precise.

1.5 Dissertation Structure

This dissertation is divided into 5 chapters beyond the introduction. The second chapter presents the basic concepts that support the work developed and give a brief review about the concepts used in this work. The review will be made in the perspective of applications for PSs.

On the third chapter, the materials used as transducers are characterised. The implications of the different characteristics for different applications is described and analysed. In this chapter, the procedures to development and assemble the sensor are explained. Details and results of tests made with sensors will be presented and analysed.

The fourth chapter describes the measurement chain and the software used. On this chapter, each module of the electronic circuit is explained and the implementation options are justified. The final prototype is presented and its advantages and issues are described.

On the fifth chapter, the results of the tests made with the final prototype are presented and discussed.

Finally, on the sixth chapter, conclusions about the developed work are drawn. The main achievements are highlighted and future work is proposed.

2. State of Art

2.1 Piezoresistivity

The piezoresistive effect is the ability of a material to change its resistance when a mechanical deformation is applied. The first person who described the piezoresistive effect was Lord Kelvin in 1856 [1]. He found that some metals change their resistivity when a mechanical load is applied. Usually, the piezoresistive event, is characterized by two electrodes and a sample of piezoresistive material that closes the circuit between them, as we can see in Figure 1. The resistance of the piezoresistive materials change with the deformation, as we can see in equation (1). In consequence, according to Ohm's law (2), current i, also changes with the deformation.

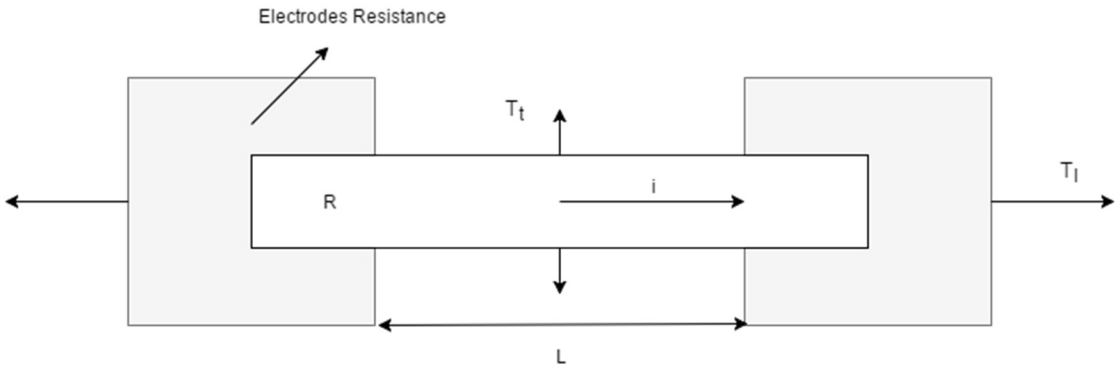

Figure 1. Schematic of typic assembly of a piezoresistive material used as a sensor.

$$\frac{\Delta R}{R} = \pi_l T_l + \pi_t T_t \tag{1}$$

where *R* is the resistance of the material, π_l and π_t are the longitudinal and transversal piezoresistive coefficients, and T_l and T_t are, the mechanical stress applied longitudinal and transversal, respectively, to the axis of the force applied to the semiconductor material.

$$V = RI \tag{2}$$

where *V* is the voltage in volts, *R* is the resistance in ohms and *I* is the current in ampere.

Later, in 1954, C.S. Smith, discovered that silicon and germanium, which are semiconductors, have a better piezoresistive behavior than metals. After that, PSs started to be fabricated from these two semiconductors. Recently, new technologies are being developed and scientists are trying to substitute silicon by polymers with carbon nanotubes (CNT) [2].

2.2 The Piezoresistive Element as a Sensor

Piezoresistive materials are used as PSs. In these sensors, the properties that make them piezoresistive are used to measure the variation of a parameter. There are different kinds of

PSs but all of them work similarly. The major difference between them are their composition and, consequentially, their electrical and mechanical characteristics. These differences give us the opportunity to apply PSs in multiple areas.

There are materials that already have piezoresistive behavior, as it was said before. However, the materials that we know now, have limitations that are inherent to their constitution. One example of this reality is that there are not known pure materials with a good relation between piezoresistivity and flexibility. Due to this limitation, we need to make our own piezoresistive materials. It's here that thermoplastic will have their main role.

Piezoresistive materials, when used as sensors, are defined by their sensitivity. The sensitivity of a sensor is given by the calculation of the gauge factor, which represents the relation between the resistance variation with the mechanical deformation. The gauge factor can be calculated by the equation (3).

$$GF = \frac{\frac{\delta R}{R}}{\frac{\delta l}{l}} \tag{3}$$

where R is the initial resistance, δR is the resistance variation during a deformation, l is the length of the sample and δl represents the deformation.

2.3 Piezoresistive Sensors with Carbon Nanotubes

In 1970, when CNT were discovered they didn't win too much credibility. Twenty years after, in 1990, a Japanese scientist used a high-resolution transmission electron microscopy to make a detailed report about these filaments. Finally, in 2003, the scientific community thought that CNT would revolutionize our technology, because it would be possible to have better computers with much smaller dimensions. Efforts have been made in this direction. However, this was not a revolution yet, because technology development is requiring additional scientific advances [3], [4].

Some scientists developed thermoplastic elastomer based composites, with CNT and polymer to produce PSs [4], [5], [6]. Some of these materials are already on the market. An example is the Velostat®, that was produced to package electronic materials, because it is flexible enough and is also an electrical conductor. These characteristics protect electronic materials from electrostatic [7]. Velostat® is made of a polymer, doped with carbon black, and because it owns a piezoresistive behavior, it is used to make experiences once this is an accessible material. Other example is the materials used by FlexiForce™ to produce their pressure sensors [8].

Composites of styrene ethylene butylene styrene (SEBS) doped with CNT are one of the methods used to produce PSs. SEBS is a polymer used as a high-performance and multifunctional material with, already proved, potential in piezoresistive materials. The SEBS material, as any normal polymer, is not an electrical conductor. This means that it only works as a piezoresistive element when is in a form of a compound. To make this possible, conductive fillers, like CNT, should be incorporated to allow the crossing of electrons in a flexible film [4], [9], [6].

CNT can have different configurations [4], [6]. For this project, a multi-walled carbon nanotube was used, as shown in Figure 2, that has the configuration of cylinders inside of other cylinders. These CNT have electric characteristics like metals and, at the same time, are lighter and smaller. The biggest issue about them in these days is that they are not easy to produce.

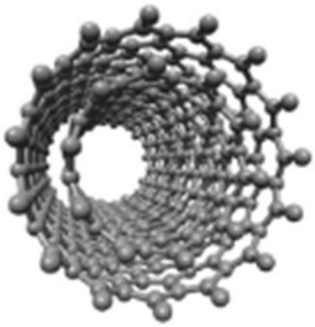

Figure 2. Illustration of a multi-walled carbon nanotube.

In this project, besides the commercial transducer, it was used a new transducer made of the composite explained on the last paragraph. Composites of polymers with CNT are a new generation of thermoplastic elastomers that already show mechanical and piezoresistive properties. This makes them excellent for applications where large deformation PSs are required. Besides that, the production of this composite uses a green solvent, Cyclopentyl Methyl Ether (CPME) that was considered by Food and Drug Administration (FDA) less toxic than the solvent used before, toluene. This is a big step in the production of sensors and enables the extension of its range of applications. Now we can use them for biomedical applications, for example. Besides, since it is possible to control the viscosity and the concentration of each compound in the composite, we can produce them with screen and spray printing technologies and with the percentage of each compound that we want. That is the biggest advantage of this kind of sensors. They make easier to obtain good quality sensor films with a lower production cost.

The biggest advantage of this kind of sensors is the production procedure and the materials. They allow us to use printing methods that make easier to obtain good quality sensor films with a lower production cost.

CNT are dispersed in the polymer, usually in small agglomerates [4]. When the polymer is with zero deformation, the CNT have a specific area and, consequently, will be dispersed in a specific way. This dispersion will be different when a deformation is being applied in the tranducer. This difference changes the number of conductive paths in the transducer and will also change the resistance. An illustration, of the behavior of composites with CNT, is shown in Figure 3. This is an example when a compression force is being applied. From the left to the right, we can observe the transducer without any force applied, and the behavior when the force is being applied.

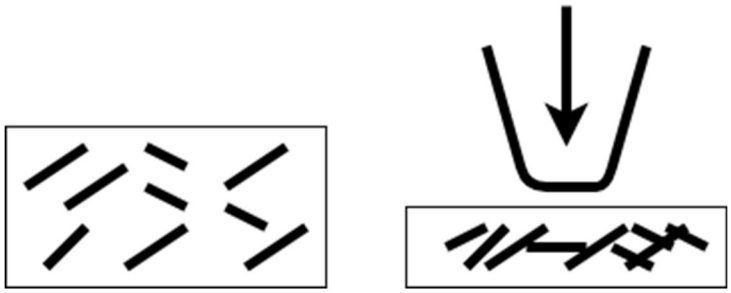

Figure 3. Illustration of a sample of piezoresistive film with CNT.

When a composite is used as a sensor, it's important to understand that we do not have a perfect solution because, when we have a composite, some properties are lost from the original compounds. In the case of the material used in this project, we have a polymer that is an electric isolator and has a big capacity of deformation, more than 200%. When the composite is made, we stop having an electric isolator. The capacity of deformation remains higher than 200%, but is also sed. The CNT, when isolated, have an excellent electrical conduction [10]. When they are in the composite, they are still good electrical conductors, however they are in low quantity and are dispersed by the polymer, what makes the composite a worse conductor, as the CNT are by themselves. The material obtained will be less flexible than the pure polymer, but has enough flexibility for most of the applications. The loss of flexibility is compensated in conductivity given by the CNT.

Finally, we can say that PSs based on polymers matrixes are not good enough to make precise measurements. Since they have hysteresis, that can change over time, when different pressures are applied.

2.4 Hysteresis

The hysteresis concept is used in different areas and defines a system in which the past events affect the future behavior. This phenomenon can be observed in thermostats, in the field of engineering [11]; in chemistry, with some chemical reactions [12]; in materials, fatigue and elasticity [4]; in biology, in cells behaviors [13]; in economics, unemployment evolution [14], amongst others [15], [16].

History about hysteresis is not completely traced yet, however in 1993, Augusto Visintin wrote a book where he merges some information about this topic. The term hysteresis, from ancient Greek, means “that which comes later”. The first time we observed this term being used was in 1882, however, this phenomenon was already described in plastic materials in 1864 by Tresca [16]. The phenomenon was studied in the ferromagnetic area by many researchers and some models to make its modulation were proposed, most of them without success. In 1935, Lord Rayleigh revised a model proposed by Weiss and Freudenreich in 1916, introducing what was called the Preisach model. The model makes a geometric interpretation of the ferromagnetism hysteresis. The Preisach model was studied by many scientists and is one of the most well-known models, however, other models were already studied to define the ferromagnetic hysteresis [15].

Plastic hysteresis started to be studied some years earlier than ferromagnetic hysteresis, in 1864. Like in ferromagnetic hysteresis, plastic hysteresis was a target of studies and different models were proposed [16]. Although all the studies and models proposed, only Bouc, , in 1966, proposed a functional approach for hysteresis. This approach was extended by Wen and a new model was presented, the Bouc-Wen model [17].

A good understanding of hysteresis can be obtained from Figure 4. A material with the behavior shown in the figure will dissipate energy every time it comes to the initial position. This happens because the response doesn’t take the same way back to the original point. To understand how the hysteresis loop works it’s important to take the following considerations.

The variables *u* and *w* are only time dependent. They can be considered system’s input and output, respectively. In an example of a pressure sensor *u* could be the force applied and *w* the voltage read.

Now that we know what each variable is, we define the paths during the increasing and decreasing of each parameter. This obviously depends on each system, but we can suppose, as example, that during the increase of the force *u*, the path that is followed is ABC and during the decrease of the force we follow the path CDA.

Supposing we start with the system in A and we increase the pressure applied, we start following the path ABC. If we go until point C and we start decreasing the force, the voltage will come by the path CDA. However, if during the increase we stop between point A and C and we start releasing the force applied, the path will be different, as represented in Figure 5, and here is where the modulation algorithms are introduced.

The center of both curves, in Figure 4, represents the energy dissipated by the material during the deformation process. The area of energy dissipation will be different depending on the

starting point. The area will also be different when the time used to apply the force changes. This because energy dissipation increases with the increase of the speed [16], [18].

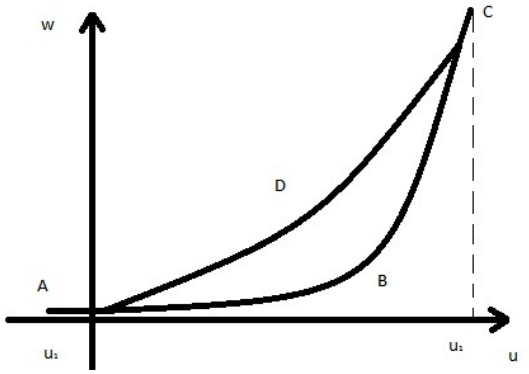

Figure 4. Illustration of a tipic hysteresis loop for an elastomer deformation.

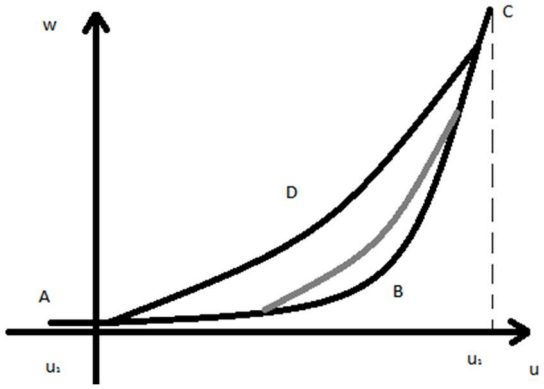

Figure 5. Behavior of an output in hysteresis loop when the direction of the input changes while $u_1<u<u_2$.

Another characteristic that the hysteresis loop should respect is that the value of the output w can only depend on $u(t)$. This means that w cannot depend on input's speed applied. This characteristic is called the rate independence memory effect and is directly associated with the hysteresis. Many hysteretic systems don't respect this rule. This is because almost all the systems are affected by the speed. In these cases, what usually is observed is that the hysteretic behavior is better defined for slower systems [1], [18].

Another situation that happens in systems with hysteresis is that the "outside" bounds are not unbreakable. For each cycle, some variations can appear, and although this can be studied, is something that increases the complexity of the hysteresis analysis.

Hysteresis can be harnessed for some applications as in cars suspensions. However, in sensors, its use can be problematic because this phenomenon causes big losses of information.

2.5 Hysteresis Models

Some sensors can be easily implemented in practical applications if they give linear responses to the inputs they receive. Other sensors don't have a linear response but can be defined with linearization algorithms. In the case of the transducers used in this work there's also another challenge, they have hysteresis. This is probably the biggest challenge when a sensor needs to be calibrated. Some engineers worked on calibration models to make possible to take information from this kind of sensors. Preisach model is an example [18]. This model was developed with focus on the physical mechanisms of magnetization to assist the study of hysteresis in magnetic materials. Other researchers started to study this model and realized that it could have other applications, beyond the area of magnetic fields. Mathematicians started to study the model and transformed it into a mathematic tool that now can be used to study hysteresis in different fields, like mechanical deformations [16], [17].

Preisach model is usually represented with a rectangular loop, as it is shown in Figure 6. The loop represents the hysteresis loop that we saw in Figure 5, where the output only considers a binary value. This value represents the state of the system if is increasing or decreasing. One of these relays is called hysteron and the system will be more precise if the number of hysterons *N* that define the systems increases. However, if the number of hysterons is too high, it will take more computational time. So, is always necessary to find a balance between resolution and performance. In Figure 6, is possible to observe that the behavior is the same explained on the hysteresis's section.

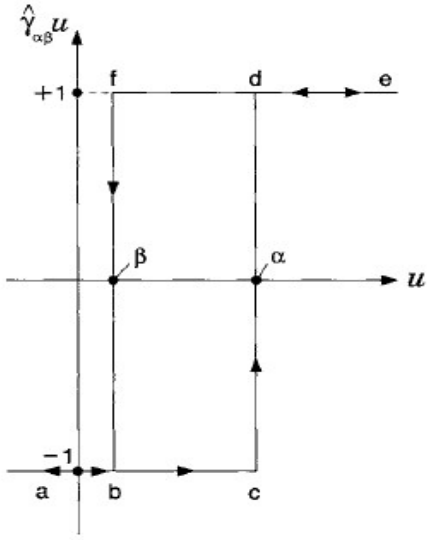

Figure 6. Illustration of the behavior of a hysteresis loop represented by a delayed relay.

In practice, if we define the behavior with only one hysteron, as it is shown in Figure 6, we will have two curves, the loading curve and the unloading curve. The first is the one defined when a force is being applied and the second is for when we are releasing the sensor.

The Preisach model is not precise when applied with only one hysteron, but if we see Figure 7, is easier to understand how Preisach model makes the modulation of the input signals when the number of hysterons increases. With the segmentation of the hysteresis loop, there is not only two curves but N curves to be considered [15], [16]. This lets the user decide how detailed he wants the system.

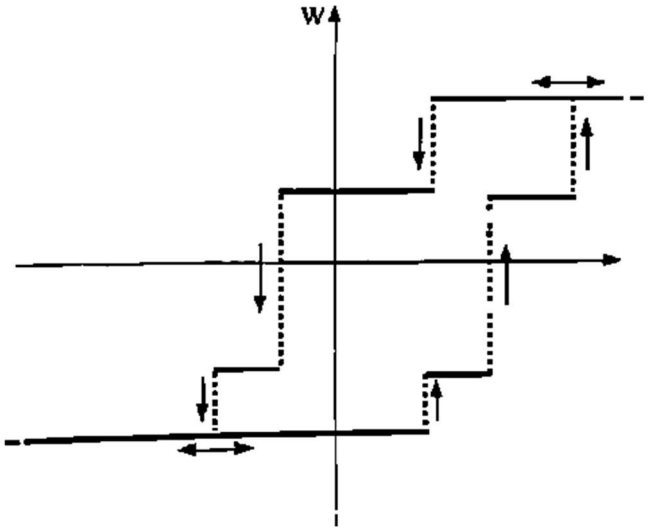

Figure 7. Illustration of the behavior of a hysteresis loop represented by multiple delayed relays.

3. Data Acquisition System

Data acquisition is the capacity of use a transducer, that converts the signal from a natural phenomenon into an electrical signal, and then reads, processes, analyzes and storages this information in a computer. On the other hand, a data acquisition system is the set of components that make data acquisition possible. Data acquisition systems sometimes are embedded with actuators, because when a phenomenon is being analyzed, usually it's not only necessary to store data for further analysis, but also is necessary to take immediate action when a specific event is detected.

The data acquisition system can be divided in 6 important elements. Sensors and transducers, field wiring, signal conditioning, data acquisition hardware and data acquisition software, see Figure 8 [19].

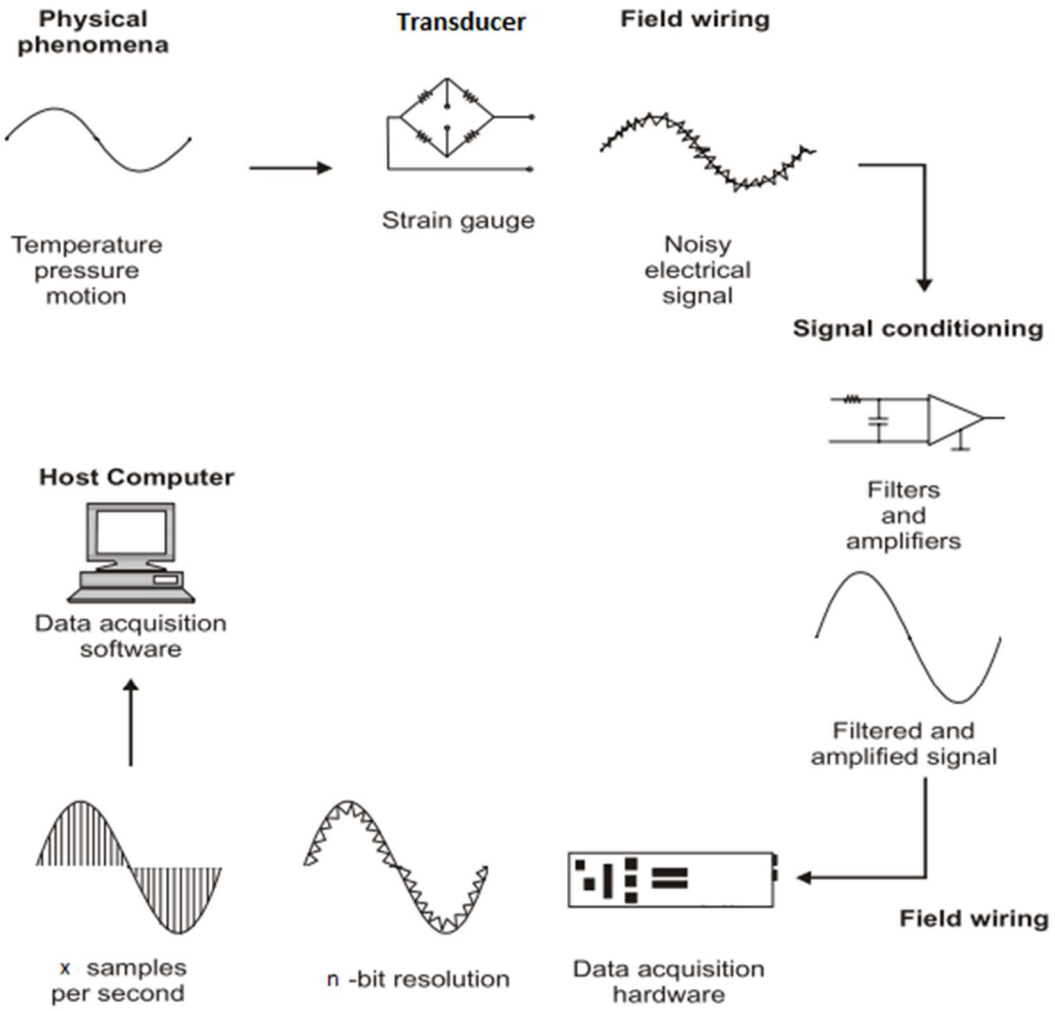

Figure 8. Diagram of a functional Personal Computer (PC)-based data acquisition system. Adapted from [11].

3.1 Data Acquisition System Development

3.1.1 Power Supply

The power source provides the energy to the data acquisition chain or other system elements, including the transducers when they are passive transducers. The achievement of a precise data acquisition system requires an extremely stable and noiseless power source. This is important because if the signal that is being processed has noise, we will get the real value affected by interferences that are not controlled. This means, if we want to say the variations we get are from the transducer and not from other sources we do not control, we must regulate it.

In this work, all the power is supplied by an Universal Serial Bus (USB) port. This source of energy can be noisy, so a low pass filter was used to clean the high frequencies noise, over 5MHz, Figure 9. This filter is applied in the beginning of the circuit, just after the 5V pin of the mbed platform.

After filtering the power supply to remove noise, we must regulate the voltage, because the measurement chain will measure voltage variations and requires a very stable power supply. The L78L33ABZ voltage regulator was used to regulate the voltage to 3.3V. We chose this voltage to maximize the resolution of the ADC, that converts input voltages from 0 to 3.3V. This decision allows maximum resolution. This voltage regulator can also supply the current need by the data acquisition system. The calculations made below are for the matrix hardware, where only the instrumentation amplifier and the digital potentiometers have a considerable current consumption:

- Instrumentation Amplifier INA333: $50\mu A * 4 = 200\mu A$;
- Digital Rheostat MAX5391: $12\mu A * 16 = 192\mu A$;

The total current requirement is $392\mu A$. The L78L33ABZ delivers until $100mA$, what is more than enough to supply the entire data acquisition system [20][21].

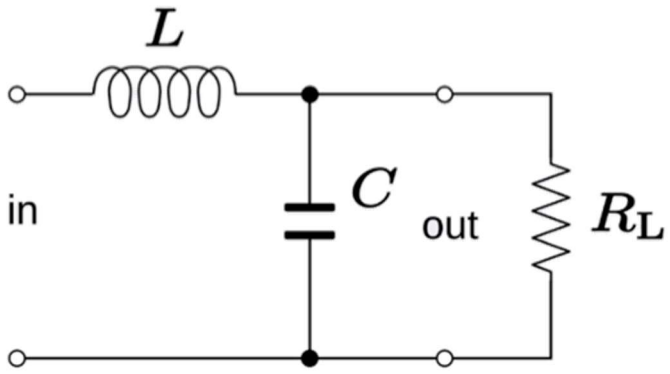

Figure 9. Illustration of the LC filter applied in the hardware of the data acquisition system. L is the inductor, C a capacitor and $R_L$is the load of the power suplly.

3.1.2 Transducers

Transducers are the components that make the interaction between the environment and the data acquisition system. These components convert one type of energy into another, they are the sensing element in a data acquisition chain. Transducers can be classified as active or passive depending on their characteristics.

Active transducers convert a non-electrical energy into an electrical signal. Because of this they don't need to be provided with a power source. The most known example of an active transducer is the thermocouple.

Passive transducers convert a non-electrical energy in a variation of an electrical parameter, i.e., they change a resistance, a capacitance or an inductance, to make the transduction. Because of that, an external excitation circuit should be provided. The transducers used in this work fit in this classification.

Transducers have specific characteristics that define the quality and the price. The most important are the accuracy, sensibility, repeatability and range [19].

3.1.3 Voltage Divider

The transducer used in the work is nothing more than a variable resistance. Resistance variation measurement can be performed using one of three well known techniques. The easiest way is to apply the Ohm's law (2). In this case, when a constant current circulates the resistance is possible to measure the variation in the voltage drop across the resistance. However, for this work, it is very difficult to achieve readable values because the voltage is 3,3V and the resistance of the transducer varies between $40K\Omega$ and $100K\Omega$. With this range of resistance and with this voltage, the current should be in the μA order.

So, because the first option is not available for this application, the second easiest method is to make use of the voltage divider, as shown in Figure 10. This circuit, unlike the previous one,

can be used in this application. With the range of values defined by the voltage and the resistances, it will be possible to have a voltage variation of at least 0.55V, Figure 11, the values were taken by the voltage divider using equation (4).

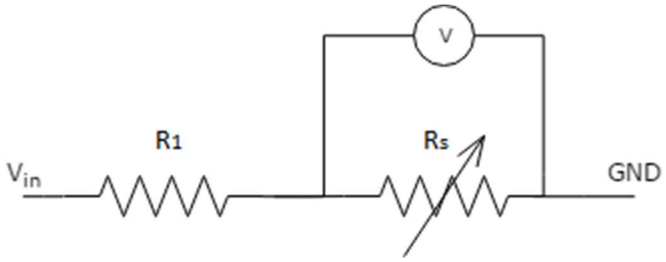

Figure 10. Schematic of the voltage divider.

$$V_{out} = \frac{R_S}{R_1 + R_S} \times V_{in} \tag{4}$$

where V_{out} is the voltage measured, R_s is the sensor, R_1 is the resistance used to tune the measurement and V_{in} is the input voltage.

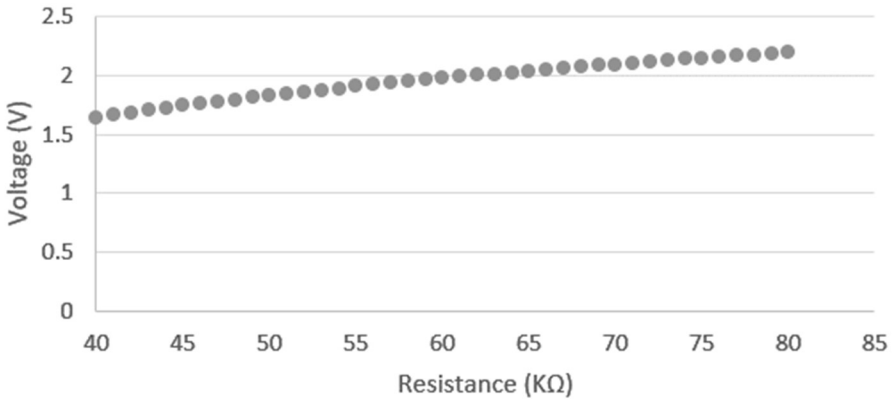

Figure 11. Simulation of the output voltage in a voltage divider with an input voltage of 3,3V.

The voltage divider is a good option to measure big variations of resistance. However, because the voltage range goes from $\cong 1{,}6$ to $2.2V$ is not possible to have a big resolution. This comes from the fact that the ADC has an input range that goes from 0 to 3.3V, so, amplifying the signal with a gain of 1.5, would give is a range of 0.9V (2.4 to 3.3V). Another problem of the voltage divider is that is sensible to noise. The voltage divider can be an option for many cases, but for situations that need more precision and better robustness to noise there is a circuit, Wheatstone bridge, that can provide better results. In this work, the voltage divider was used to in most of the experiments, because it's easier to calibrate and doesn't get out of range so easily as Wheatstone bridge.

3.1.1 Wheatstone Bridge

In 1833, Samuel Hunter Christie invented a circuit that was capable of discovering the value of an unknown resistance using three other resistances with known values. Ten years later, Sir Charles Wheatstone improved the circuit and made it popular in the engineering society.

The Wheatstone bridge, consists in a four resistances circuit, that can be represented as shown in Figure 12, and it's used in multiple applications, the most well-known are in instrumentation devices. The Wheatstone bridge has advantages that makes it the preferred method for many applications.

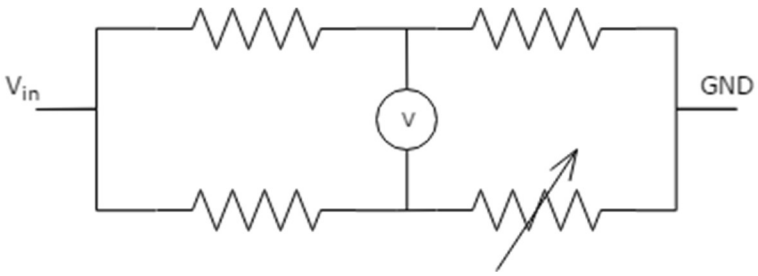

Figure 12. Schematic of the Wheatstone bridge.

The bridge circuit is highly sensitive to small resistance variations, and besides that, is not affected by noise from the power source. This happen because the common mode of each arm of the bridge is cancelled, as shown in (5). That's one of the most important advantages of Wheatstone bridges.

$$V_{out} = \left(\frac{R_S}{R_1 + R_S} - \frac{R_3}{R_2 + R_3} \right) \times V_{in} \tag{5}$$

where V_{out} is the output voltage, R_s is the resistance of the sensor, R_1, R_2 and R_3 are the correspondent resistances in Figure 12 and V_{in} is the input voltage.

Another important parameter to control is the sensitivity of the measurement chain. For the Wheatstone bridge, the sensitivity is another important parameter and is defined by the relation between the variation of the output voltage and the variation of the sensor, equation (6).

$$S = \frac{\delta V_{out}}{\delta R_S} = \frac{V_{in} R_1}{(R_S + R_1)^2} \tag{6}$$

where *S* is the sensibility, V_{in} is the input voltage, R_1 is the fixed resistance and R_s is the sensing element resistance.

The sensibility of the bridge circuit is the same as the voltage divider, it only depends on the arm where the sensor is. Moreover, because there's not offset, as we can see in Figure 13, is possible to apply higher gains to the signal and, thus, achieve increased resolution.

When a gain is applied, the sensibility will be proportional to this gain, equation (7).

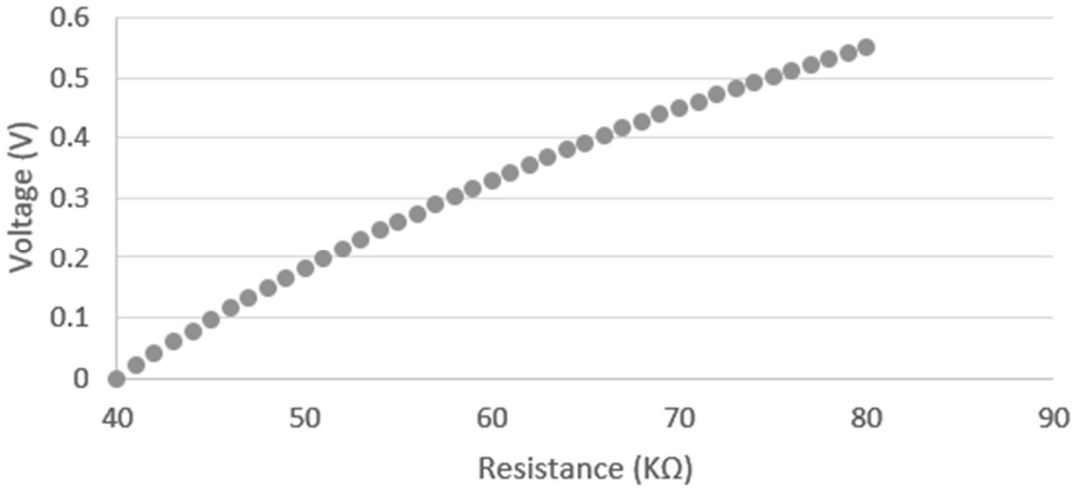

Figure 13. Graphic representing a simulation of the output voltage in a Wheatstone bridge with an input voltage of 3,3V.

$$S = AV_{in}\frac{R_1}{(R_S + R_1)^2} \tag{7}$$

where *A* is the gain, V_{in} is the input voltage and R_1 and R_s are the resistances fixed and sensor, respectively.

With this circuit, for the same sensor is now possible to apply a gain of 6 and this will give a maximum voltage of 3,3V, this means a range from 0 to 3,3V. This is the maximum resolution that can be taken from the ADC.

As shown in equation (7), the sensibility change depends on the fixed resistances. This means that, if the fixed resistances are changed by digital rheostats is possible optimize the signal acquisition for different sensors. For this work, both, the voltage divider and the Wheatstone bridge have rheostats instead of fixed resistances.

Unbalanced Bridge

While a Wheatstone bridge is operating, the sensing resistance varies, this means that in most of the time, the circuit is unbalanced. When this happens, the voltage V, Figure 12, is different from zero. The measurements of voltage during experiments is always based on this voltage variation. This means that there are at least two possible ways to calculate the resistance of

the sensor. The first one, is measuring the voltage and make the calculations, the second is changing one of the resistances of the arm until the voltage is zero [19].

3.2 Signal Conditioning

The signal conditioning is important in data acquisition systems. It ensures the signal that is being collected is not affected by noise until it arrives the data processing module. This step is very important when a signal is being acquired in noisy environments.

Noise it's one of the biggest problems in instrumentation devices. It can have origin from inside or outside the acquisition system, the power source, other electrical devices working near or even by near electrical cables that are carrying different signals.

A signal conditioning circuit performs the following operations in the signal: amplification; isolation; filtering; excitation and linearization. Here only the methods used in this project are detailed.

3.2.1 Amplification

Amplification main's functions is to increase the resolution of a signal and the signal-to-noise ratio. When the signal is properly amplified, the magnitude of the signal acquired is increased to a higher level. With this, the signal can cross a noisy area because the effect of this noise will be irrelevant considering the difference of magnitude of both signals [19]. In this project, all the signals are amplified to an optimized gain that gives a maximum resolution.

3.2.2 Filtering

Filtering a signal is the action of removing the noise before it can be misinterpreted with the acquired signal. This can be made through different ways, as it is possible to see in [19]. However, for this work, besides the filtration that was made to the excitation voltage of the measurement chain, the averaging method was implemented. This method consists in the acquisition of more samples than necessary, and performing an average. The noise influence should be eliminated after the application of this method. When is not possible to make the filtering by software, the alternative is to do it using an analog filter.

3.2.3 Linearization

As it was shown in the chapter about hysteresis, some sensors don't produce a linear output. However, if the non-linear variation is repeatable and predictable the linearization can be made before the signal storage. This requires computational capacity, so it's only possible to apply with smart sensors, where a micro controller unit (MCU) can make the linearization before sending the data to the user.

3.2.4 Data Conversion

In this section of the data acquisition system, the analogic signal is converted in a digital signal. We should be aware that this procedure introduces a loss of information. This loss doesn't mean that the work can't be done, if all the special details can be observed, then the digital signal is a good representation of the original analog signal.

The component used to make the conversion between the analog signal to a discrete signal is the analog to digital converter (ADC). The ADCs can have different resolutions; this characteristic is defined by the minimum variation that it can detect in the input. For example, in this work, the ADC used was a 10-bit ADC that converts voltage from 0 to 3,3V, i.e., it will give us values from 0 to 2^{10}-1 where each increment means a difference of $\cong 3{,}2227$ mV. In this case, any variation on the input lower that this value will not be detected.

3.3 Communication

At this point, the information to build the data acquisition system is almost described. The excitation power for the measurement chain was characterized and the signal conditioning was explained. Now, it is necessary to find a solution to gather the signals from a group of sensors and put all this information in the MCU. With the information, available in the MCU, data is processed and sent to the computer where it can be analyzed trough the user interface. This communication, between the different components of the data acquisition system, needs to be coordinated in a way that, at the end of the day, we can know what information we received and from where this information came from.

3.3.1 Microcontroller to Element Sensor

We already know that the signal is converted from analogic to digital by a 10-bit ADC. However, there are multiple sensors connected to the same data acquisition system. To manage this situation, a low voltage 8x1 multiplexer was used [22]. This multiplexer works with logic ports to switch between the sensors. So, to do this communication, the MCU sends the values depending on the sensor to read. Because the firmware in the MCU chooses the sensor, it always knows from where the signal comes from.

3.3.2 Microcontroller to Digital Rheostats

Rheostats were used to improve the sensibility as explained in chapter 3.1. The digital rheostats MAX5393 MAUD were selected for this project because of three main reasons. First, they are accessible by Serial Peripheral Interface (SPI) communication protocol, which makes it possible to be used with the mbed. Second, they have a resistance of 50KΩ that can be defined by an 8-bit configuration message, what gives 256 different tap points, i.e. about 195Ω of precision. Finally, they have a low quiescent supply current what is always a good choice for low power applications [21].

3.3.3 Serial Peripheral Interface Communication

The SPI communication protocol is very used in embedded systems. This protocol has one master and several slaves, i.e., with one MCU we can have several devices connected at the same time, depending only on the number of digital ports available on the MCU.

This communication protocol connects two devices through three or four lines. The two devices are called the master and the slave. The Master has two special roles. First, defines the serial clock frequency in the line clock that is usually denoted by SCLK. Second, chooses which slave will be open to communicate, using the chip select (CS) line. The other two lines are the Master In Slave Out (MISO) and the Master Out Slave In (MOSI) used for data exchange among the Master and the Slave. The MOSI is, the line used to send messages from the Master to the Slave, and MISO is used to send messages from the Slave to the Master. In some devices, as is the case of the MAX5393 used in this work, there is not MISO. This means that any information is sent from the rheostat to the MCU.

As shown in Figure 14, the SPI communication starts putting low the CS line. All the communication is made while this line is in the low state. At the end of the communication, the CS line will return to the high state. The SCLK is always sending the clock signals used to synchronize the communication. In the example, we can see that the reading moment happens at the rising hedge of the clock signal, i.e., the hedge demarked with arrows on Figure 14 Finally, the MOSI line will send the message and, each time the clock signal goes up, a new value is taken from this line until the CS goes low again. The Slave will interpret the message as it is built or programmed to. For example, the device used in this project receives a 10-bit message. The first two bits are to define which rheostat we want to change and the remainder bits store the value of the rheostat.

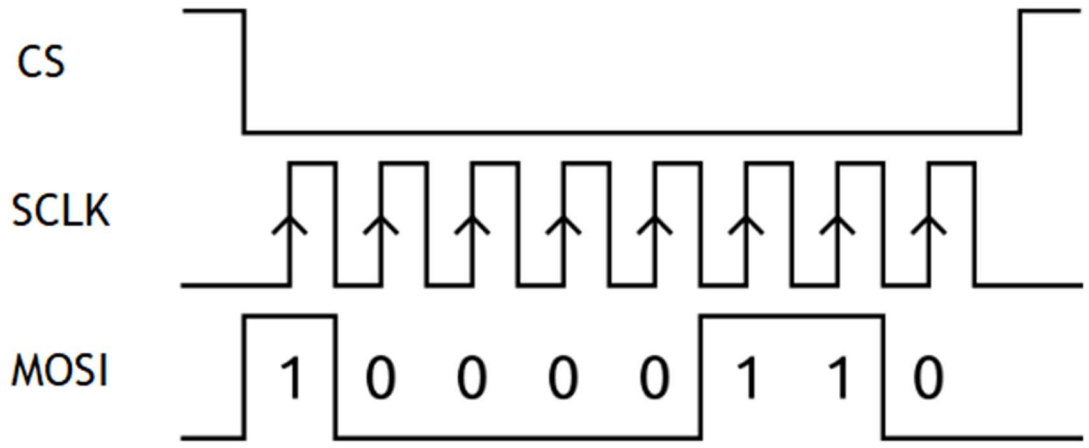

Figure 14. Illustration of the SPI communication.

3.3.4 Microcontroller and Personal Computer

To make the communication between the MCU and the computer, two versions were developed, one wired and another wireless. Wired communication was developed with the serial communication that uses the USB port from where the MCU is powered. The wireless communication was implemented with the module Wi-fly RN-171 as it will be explained in sub-section 3.6. Although we have tested different ways of communication, the message structure is the same.

At this point it's important to understand how the information is processed after being converted by the ADC and before being sent to the computer.

First, we know that the mbed platform already represents the value converted by the ADC in the floating-point format, with values between 0 and 1. This means that for values $\leq 0V$ we have a value of 0 and for values $\geq 3{,}3V$ we have the value 1, the intermediate values are discretized in 2^{10} steps.

The message sent by the serial port is sent as bytes. Information that comes from the MCU to the PC includes data to identify the sensor and the value of the sensor. Information that flows from the PC to the MCU can be, an order to start/stop the data acquisition an order to calibrate the data acquisition system or to tune the precision that we want on the measurements. All these methods, can be adapted and more functionalities can be added depending on each situation.

MCU to PC protocol

Each message sent by the MCU has the following information about the sensor:

- ID number;
- Voltage value.

The protocol data structure has 4 bytes of length, as shown in Figure 15. The first byte is the starting byte and was defined as 0xFF, this byte notifies the receiver that a new message is arriving. The second byte lets the computer know which sensor was measured. Finally, the last two bytes are reserved for the voltage value that comes in a 16-bit format. The byte number 2 carries the most significant 8-bits of the voltage value and the byte number 3 carries the less significant 8-bits.

byte 0	byte 1	bytes 2 and 3
0xFF	Sensor ID	Voltage value

Figure 15. Buffer of data sent by the MCU to the PC.

For example, if we want to send to the PC the voltage of sensor 2, the value returned by the ADC is 0.49587. The first two bytes that will be sent, take the value 0xFF and 0x01. The last two bytes are calculated as following.

A value of 0.49587 results from the conversion process performed by the ADC when the input applied is 1.636371 V. We need to send this input as an integer with the biggest resolution possible. To do so, we proceed as described next.

First, we take the value 0.49587 and multiply it by 3.3 to transform it in the real value of voltage (8).

$$v = in \times \max_v \tag{8}$$

where *v* is the voltage at the ADC input, *in* is a value that goes from 0 to 1, received by the MCU, and max_v is the maximum voltage that the ADC converts on the full-scale.

After this point, we have a value of 1.636371, that is located between 0 and 3.3V and is representative of the ADC input. Now, it is necessary to transform *v* in an integer between 0 and 65536, that is the maximum value that we can carry in 16-bits message. To do this we need to multiply v in such a way it only goes until 65536, as shown in equation (9). Once v has as maximum value 3.3, we can multiply it by 10000. This will give us a value to send between 0 and 33000. This doesn't give the best resolution but already give us a good range of values.

$$v = v \times f \tag{9}$$

where *f* is the multiplication factor. At this point, we would get the value 16363 to send.

As we send values in 8-bit messages we must divide the voltage value by 256 (2^8) and then save this value in byte 2 (10).

$$b_2 = \frac{v}{256} \tag{10}$$

After this calculation, we have the value 63 to put in byte 2. Then with equation (11) we calculate the value that will be sent in byte 3. In this case, will be the value 235.

$$b_3 = v - (byte_2 * 256) \tag{11}$$

In the example, byte 2 and byte 3 will be 0x3F and 0xEB, respectively. Finally, the data structure received by the PC would be: 0xFF 0x01 0x3F 0xEB.

PC to MCU protocol

The information sent by the PC to the MCU has the following data:

- Type of order;
- Value of the order (if applied).

The protocol used to make this communication follows the same philosophy as the communication from the MCU to the PC. In this case, the buffer, as shown on in Figure 16, is a 4-bytes' buffer too. A starting byte is also sent, followed by one second byte, that will let the MCU know which kind of order is being sent and, finally, the last two bytes tell which is the value of the order.

byte 0	byte 1	bytes 2 and 3
0xFF	Order ID	Order Value

Figure 16. Buffer of data sent by the PC to the MCU.

The simplest example is the order to start/stop an acquisition. Supposing that the orders to start/stop are defined by the identifier 0x01 and inside these orders list the order to start is defined with 0x01 and the order to stop as 0x02. The buffer structure will hold; 0xFF 0x01 0x00 0x01, to give a start order to the MCU.

3.4 Reading Algorithm

At this moment, there is a sensing element, connected to a measurement chain that is incorporated in a complete data acquisition system. We have a computer receiving data from sensors and, the computer, for its part, can send orders to the data acquisition system. If the project had stopped on this point, it would be possible to have a sensor that could detect deformations and would present the results in a graphic. However, as it was explained in chapter 2, the sensors used for this work are not linear and besides they also have hysteresis. Therefore, a reading algorithm is needed to make a better approach of the sensor's answer. For this work, an adaptation of the Preisach model were implemented to improve the results of the sensors response.

3.4.1 Hysteresis Modulation

In Figure 17, is shown an example of a hysteretic behavior found in one of the sensors used in this project. The modulation must take in account the Preisach model. All the calculations and alterations to the signal have the main goal of putting the signal in a domain that fits in the algorithm already developed to apply in ferromagnetic hysteresis [23].

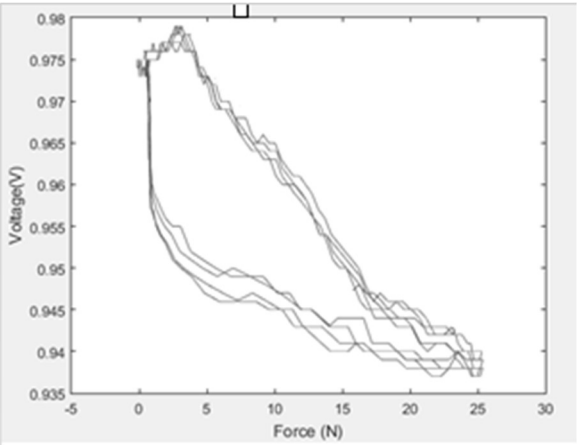

Figure 17. Graphic of force vs voltage of the non-commercial piezoresistive transducer.

The steps that need to be followed are the definition of the maximum loop, i.e. the loop which has the maximum hysteresis, blue dots in Figure 18, the calculus of the weight matrixes and calculus of the hysteresis loops that we want to test, that are the information needed to trace the red dots. In the end, the algorithm will take the maximum loop and, depending on the maximum definition chosen by the user, it will give an approach of the output expected. A sample of the output expected is shown in Figure 18.

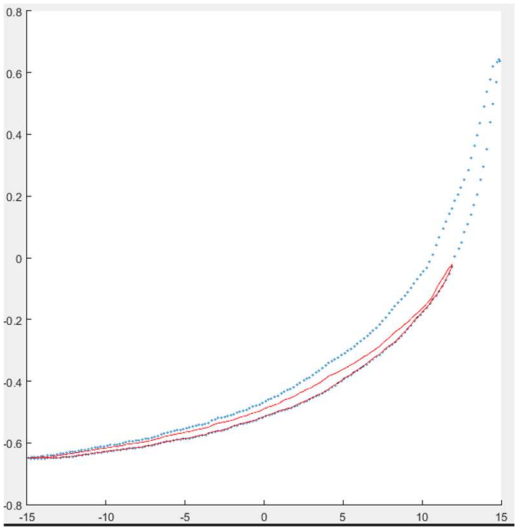

Figure 18. Example of the final result of the preisach model.

Before starting to define the maximum loop, some samples should be taken. Afterwards, these samples are used to make an interpolation to define the Preisach function (maximum loop). After getting the function, it is necessary to calculate the triangular matrix. To accomplish that, we need to make use of four supporting matrixes. These matrixes, save data like the initial values, the markers and the final matrix. The main goal of this process is to define the way the output will behave. After that, it is possible to define the path of the output for a given input [23].

The algorithm will calculate the output for a given input using the matrixes that were calculated before. For systems with a big range of hysteresis this can reduce the error margin, since it takes in account, not only both curves of the hysteresis function, but also divides itself in the number of curves that we decide at the beginning of the algorithm. As expected, the number of curves used to define the model can compromise the execution time of the algorithm. We tested for a *N* between 1000 and 2000 and we could conclude that this is a good value of *N* for the way this code is implemented.

3.5 User Interface

For a better use of the platform, a user interface was developed in Processing. This software makes use of the communication protocol explained in chapter 3.3 to give us the answer of all the sensors in real time. For this work, we used two different styles. The first one, shown in Figure 19, presents in a graphic the answer of three sensors. This was used to help during the analyze and characterization of the behavior of the sensors. In the second graphic interface, we have a colored map with eight isolated squares, Figure 20. Each square represents a sensor element and the colors change depending on the pressure that is being applied on the sensor. This interface was made only to show the interaction of the sensors. Colored maps are used in many applications with PSs that are already on the market. This is a good option when we are making a qualitative measurement.

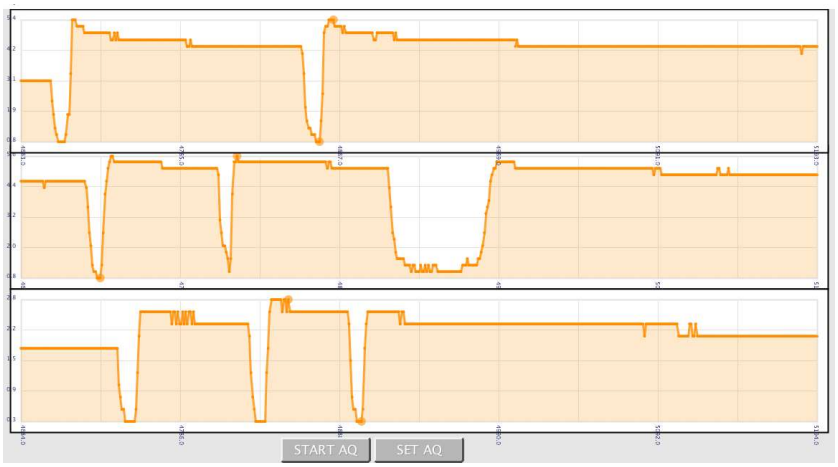

Figure 19. User interface, presentation of the answer of three sensors in a line graph.

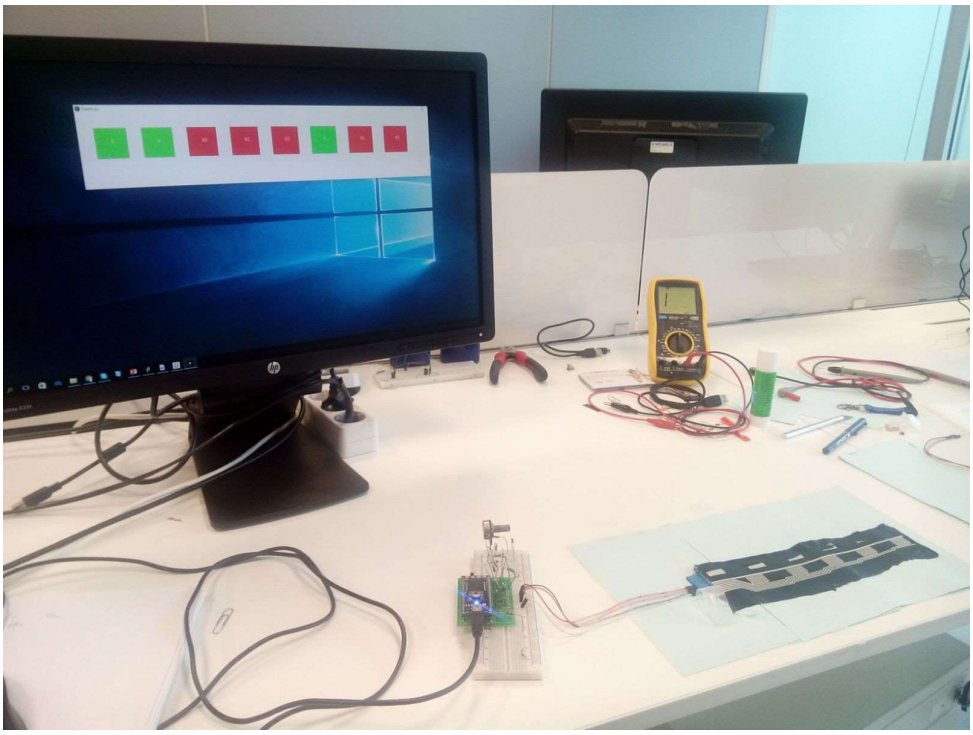

Figure 20. User interface, presentation of the results in a color map.

3.6 Hardware Development

After the development of the prototype, assembled on the breadboard, shown in Figure 21, three versions of the hardware platform were developed, all of them were based in the mbed platform. The prototype has three voltage dividers, each one can read the value of one sensor. It doesn't have any protection against the noise and it is necessary to tune the rheostat occasionally to keep the voltage divider as sensible as possible. Although this was the first prototype, the results from the tests made with it were interesting. This was a good version to make the first tests because it is easy to calibrate and it can be calibrated directly on the hardware.

The first version board, Figure 21, only allows the user to use a Wheatstone bridge. One improvement that this board introduced in relation to the initial prototype is that it's less sensible to the noise. Other improved part is it uses of a multiplexer to measure all the transducers by the same data acquisition chain. Finally, we can say that this version of the board is not flexible and only let us use a specific transducer with a specific base resistance. It's possible to see the first version of the board in Figure 22.

The second version of the board, Figure 23, is like the first one, with three major improvements. First, instead of fixed resistances we have digital rheostats. This gives the opportunity to have a board adaptable to sensors with different rest resistances and makes it possible to control the resistance through a software. The second main improvement is that we gave the opportunity to the user to choose between a voltage divider and a Wheatstone bridge.

This is done manually by switching a jumper. Finally, the gain of the signal can be variable too, and it can also be defined by software.

The breadboard prototype and the version 2 of the board were the ones which were used in the tests presented in the results chapter of this work.

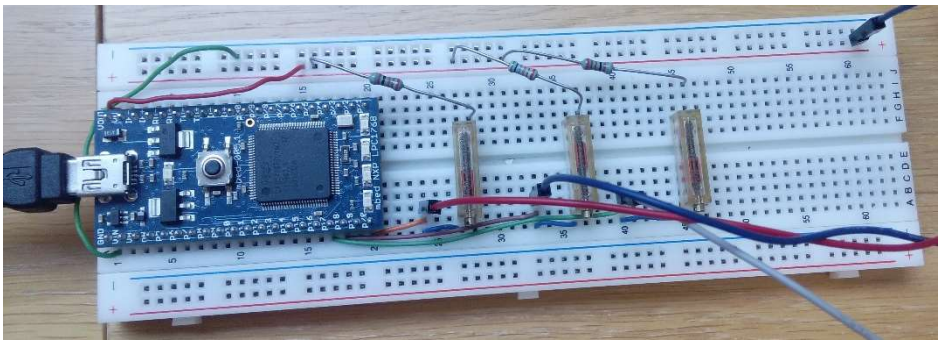

Figure 21. First prototype of the data acquisition system.

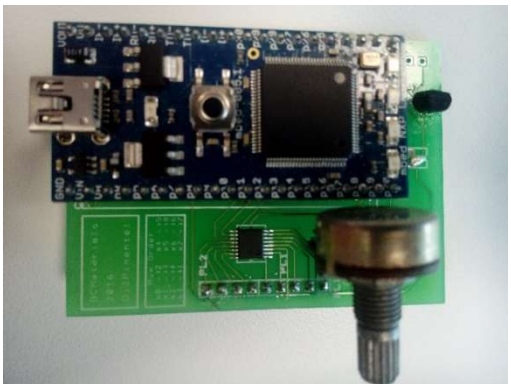

Figure 22. Printed circuit board (PCB), version 1.

Figure 23. PCB, version 2.

Finally, a third version of the board was designed, Figure 24. The data acquisition system, in this version, is like the version 2, however, this one has hardware to receive information of up to 32 sensors at the same time. This version has another improvement relatively to its previous one. Pins were reserved to make use of communication by wireless, using a RN-171 wi-fi module. Bugs that were detected in the older version were fixed too.

The main goal of this version is to understand how to manage a higher number of sensors by software. This is the most improved version and it's the one that shall be used in future works.

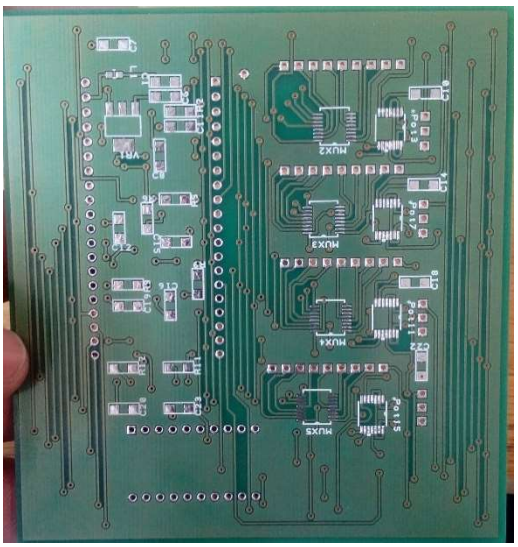

Figure 24. PCB (back side), version 3.

The mbed platform

The mbed LPC1768, Figure 25, is a 32-bit ARM MCU and is used to rapid prototyping. The platform supports USB, Ethernet, CAN, Serial, I2C and SPI communication, and gives to the user a PwmOut, AnalogIn, AnalogOut, DigitalIn and DigitalOut pins that are enough for applications like this work. A built-in USB flash programmer is included to. The web platform already provides several libraries that give to the user the opportunity to work faster once there is an abstraction layer that improves the development speed [24].

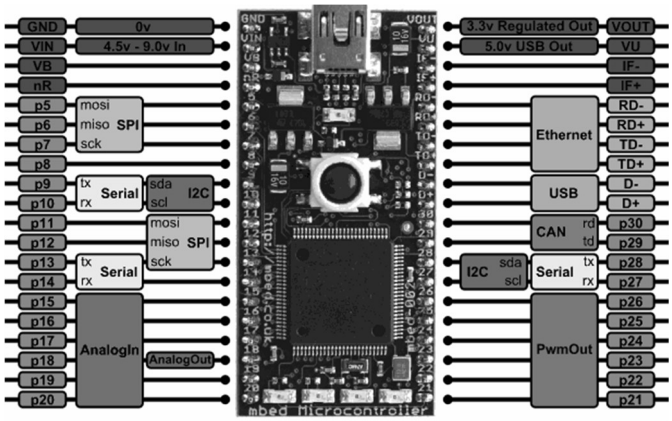

Figure 25. Pinout of mbed LPC1768 hardware.

Wifly RN-171

The wifly module RN-171, Figure 26, was used in version 3 of the board. Besides all the capabilities of this model that can be found in its documentation, we only used the module to send the same data that was sent when the wi-fi was unavailable in the previous versions. Some of the characteristics that are important to give reference for this project is that it can connect to WPA-PSK networks and it has a low energetic consumption [25], [26]. The module was used only as a demonstration of the wi-fi potentialities. However, in other versions of the hardware, it is possible to make use of the analogic ports to read more sensors at the same time or to create an ad-hoc network.

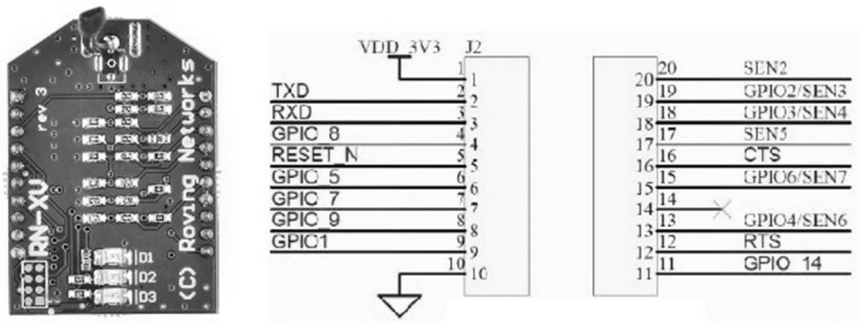

Figure 26. Illustration and pinout of the wi-fi module, RN-171.

4. Piezoresistive Transducers' Characterization

4.1 Materials and Methods

Two kinds of transducers were tested, the first one is a noncommercial transducer developed by the Smart Material Research Group from the University of Minho, and the second one is a commercial transducer, FSR 400 (Interlink Electronics®). The basic process to produce this kind of transducers is similar for both, however there are some different assemblage methods that can make the difference in the final product.

4.1.1 Noncommercial Transducer

The noncommercial transducer was produced in the laboratory during this project. To produce it, the materials used were: multi-walled CNT, CPME and SEBS. All of them already explained in chapter 2.3.

Beginning by the preparation of the transducer film, Figure 27, the process starts with the dissolution of multi-walled CNT with cyclopentyl methyl ether (CPME). To maximize the dispersion of the multi walled carbon nanotubes (MWCNT) it's necessary to put the solution under an ultrasonic bath for at least 6 hours. During this time, the sample must be kept in cold water, if not the solvent will evaporate before the end of the dissolution. After the dispersion of MWCNT it is expected to obtain a black homogeneous solution. Then, SEBS is added to the solution and everything is magnetically stirred, this last step dissolves the SEBS particles giving a homogeneous viscous solution. Finally, the solution is spread homogeneously in a clean glass. For this project, we made a film with a thickness between 50 and 300μm. After the film is on the glass, it is left to dry until all the solvent evaporates. In the end, a plastic black film should be obtained, as is shown in Figure 27 in the 5th step [4].

At this point, the transducer is already prepared, now it's necessary to make the electrodes. To produced them, a polymer matrix and plate ink were used. Through screen printing technique, the plate ink is deposited over the polymer matrix with the desired configuration. Then, to finish the process, the electrodes, already deposited on the polymeric matrix, stay in an incubator at 60ºC for half an hour. The result, is a polymer matrix with plate electrodes over them like it's shown in Figure 28.

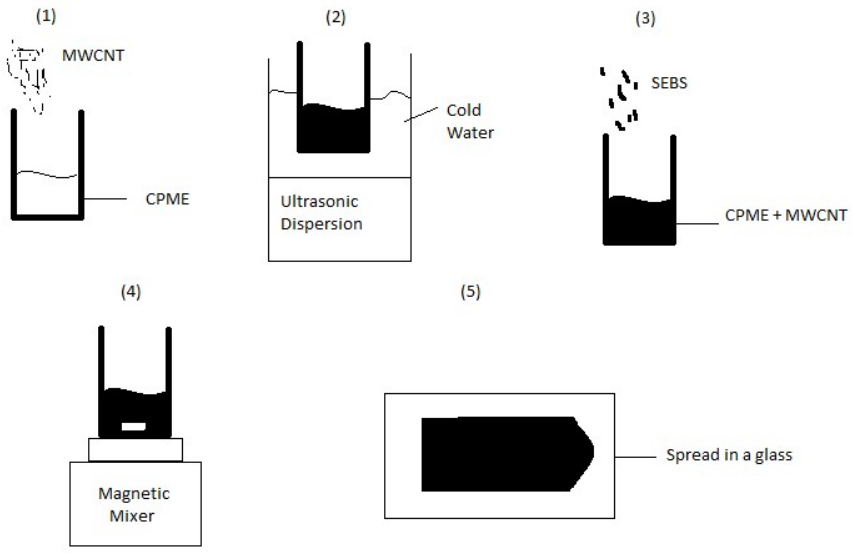

Figure 27. Preparation of a Transducer film sample. Step 1, add MWCNT with CPME. Step 2, ultrasonic dispersion. Step 3, addiction of SEBS. Step 4, magnetic stirring. Step 5, spread the solution in a glass in the desired width.

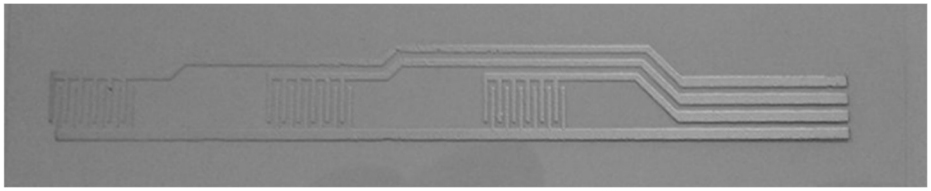

Figure 28. Sample of the polymeric matrix with printed electrodes.

After the last two steps, we have the electrodes on a polymeric matrix and a film of transducer. Now, it's necessary to make the assemblage of both components. A good connection between the transducer and the electrodes is extremely important. The importance of this step can be explained from an electrical point of view, with Figure 29. After being assembled, the transducer must be the only resistance between the two terminals of the electrodes. However, this only happens in an ideal assemblage. As it's possible to see in Figure 29, the equivalent circuit has other two associated resistances that will change depending on the method of assemblage. These connections between the transducer and the electrodes must have the lowest possible resistance. Besides that, these resistances should not change over time. If the electrodes are not making a good connection with the transducer, new variables are added to the system and new errors will be associated.

For the assembling of the transducer it was applied a method, which consist in the deposition of layers, Figure 30. To accomplish this, each layer of the film was cut in the desired lengths and then put over the electrode layer, as shown in Figure 30.

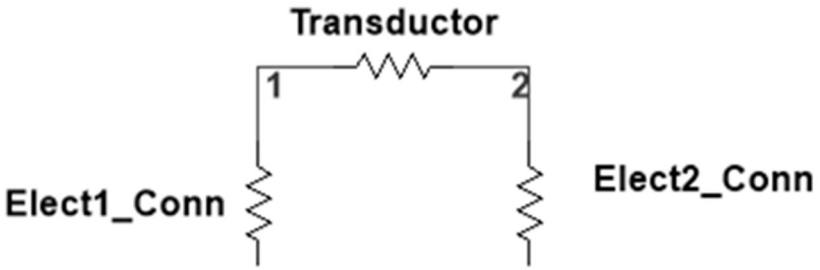

Figure 29. Equivalent circuit of the connections between the transducer and the electrodes.

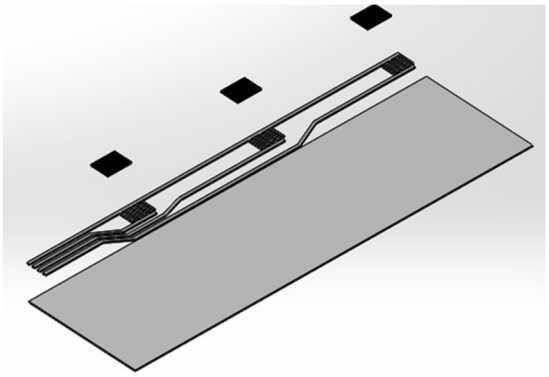

Figure 30. Illustration of the assemblage of the transducer with the electrodes with the application of pressure to join each layer.

To protect the film, a layer of polymer matrix was put over it. This polymer matrix is the same used in the bottom layer, where the electrodes are deposited. For this work, this polymer matrix is considered uncompressible. The result at this point, is a complete sensor element, that is made of three layers. The first layer is a polymer matrix with electrodes deposited in its surface, which make the second layer. Finally, a third layer contains the transducer samples. Figure 31 shows a photo of the final sensor transducers.

One more assembling method was tested, Figure 32. This time, instead of making the electrodes separately from the transducer, the electrodes were directly deposited over the transducer film. This method gives more freedom and it's easier and faster to implement. However, because the plate ink is not as elastic as the transducer, it brakes when a deformation is applied, what changes the resistance of the electrodes in a way we cannot control, Figure 33. Other situation that was found with this kind of assemblage is the fact that we don't have a division between all the sensors, Figure 32. This could not be a problem because the resistance of the piezoresistive polymer is much higher that the plate ink. However, in practice this jeopardizes the measurement and reduces the sensibility.

At the end, whatever method we use, the transducer and the electrodes should be assembled in a way that the best possible connection with each other is established. Then the electrodes are connected to the data acquisition platform, that will read and process the data received.

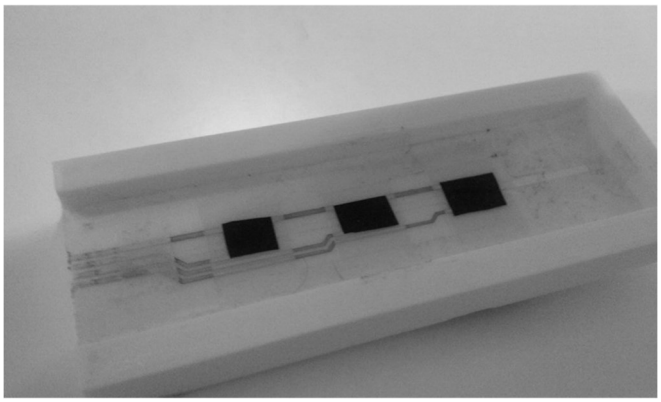

Figure 31. Electrodes with samples of transducer forming an array of sensor.

Figure 32. Image of a sample of a PS array with the electrodes printed directly on the film.

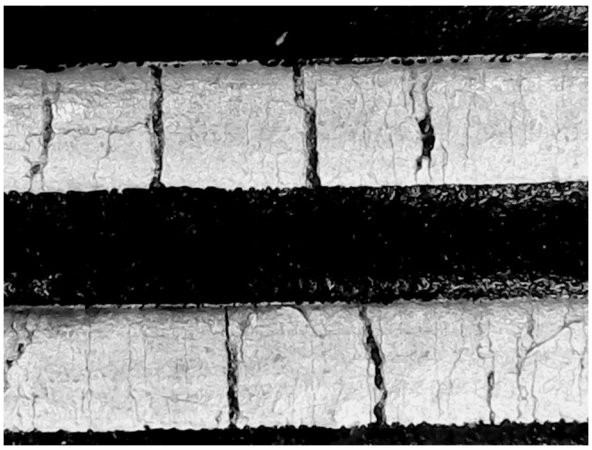

Figure 33. Microscopic image of the electrodes after being put under a deformation.

4.1.2 Commercial Transducer

Detailed information about the materials and methods of production of the commercial transducer aren't available. However, the information accessible from the manufacturer, illustrated on Figure 34, shows that the process is similar with the one used to produce the noncommercial transducer. It is possible to see that there is a small difference, for example, there is a spacer adhesive in one of the layers. This spacer ensures that when any pressure is being applied to the transducer, it will not be touching the electrodes. This can be a good

solution because while the transducer is not being pressed energy is not being wasted, once the circuit is open. In Figure 35, there's the commercial sensor element already assembled [27].

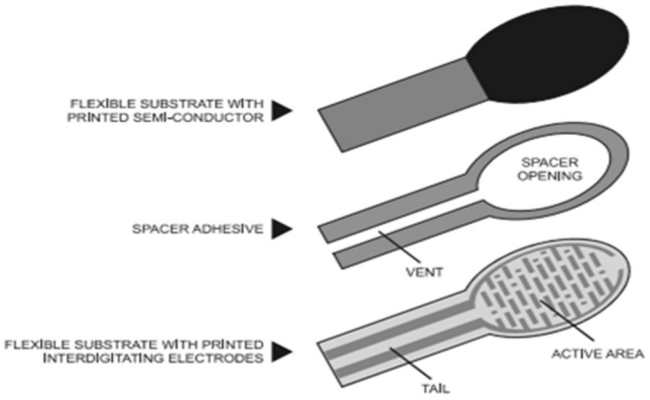

Figure 34. Illustration of the assembling of the commercial transducer [27].

Figure 35. Illustration of the commercial transducer assembled [27].

4.2 Characteristic Curves

4.2.1 Tests

To work as a sensor, a transducer must produce repeatable and must have a well-known long-term drift. The first one is easy to understand, a sensor is not good enough if it doesn't give consistent data, i.e., for the same input it shouldn't change the output over the time. The long-term drift is the variation that the sensor has in its behavior during the time is being used.

Although the samples used in this project were already tested when developed [4], it's important to test them again in this work, but now in conditions that are closer to the ones in real application. In [4], stretch tests were made. However, it's necessary to do compression tests too. To accomplish the goals of the tests, different samples were used and characteristic curves were traced. We tested the commercial and the noncommercial transducers, and then the results were compared.

4.2.2 Commercial Transducer

In the case of the commercial transducer, it's known that the repeatability is $\pm 6\%$ and the long term drift is $< 5\%\ per \log_{10}(time)$ [27].

For this sensor, the test consisted in a force which was applied cyclically. The speed of response, the repeatability and the hysteresis were analyzed.

4.2.3 Noncommercial Transducer

In the case of the noncommercial transducer, it's known that the sensor starts being repeatable after ± 100 cycles but a long drift term is not specified.

The noncommercial transducer was subject to more tests than the commercial one. The tests made with the noncommercial transducers had as main goal observing the behavior in three different situations. After the stress of cutting and manipulating, after some resting time and after be under a deformation. The deformation test, can also be divided in two, one where the force was applied in cycles and other one where the samples were submitted to discrete deformations.

After the assembling, one array of three sensing elements was left resting for 19 days. Two of the sensors were left connected to a power supply with 3.3V, the third was left disconnected from any circuit. It was expected with this test to check if the handling of the samples would affect the resistance and if the resistance would change with the resting time.

After that time, it was observed that, transducers which were connected to the power source, decreased 19% of their resistance, the transducer that was left disconnected decreased 13% of its resistance. An explanation for this event can be related with the temperature. Once this test was made at room temperature in winter season, the heat from the cross of current could let the sample to adjust better than the one that was disconnected.

After the resting test, the sensors were submitted to tests of compression. In these tests, a force was applied cyclically, increasing and decreasing in continuous cycles using the squeezer that is shown in Figure 36. Tests were performed where the forces were applied in a discrete way too, Figure 37.

The first deformation test applied in the sensors was with discrete weights. With metallic weights of 130g. By the equation 2.1 we can conclude that for one weight we have 1,27N.

$$F = m * a \qquad 2.1$$

where F is, the force applied, m is the mass in kg and a is the gravitational force $\pm 9{,}8 \mathrm{ms}^{-2}$.

Figure 36. Illustration of the test made with cyclic forces.

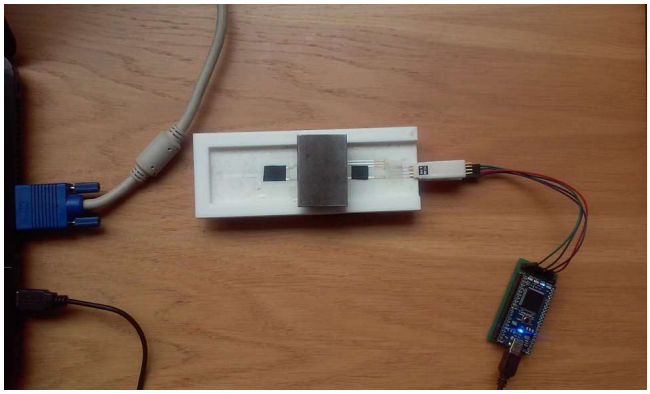

Figure 37. Illustration of the test made with discrete weight.

All the tests made with the noncommercial transducer, were made with an array of 3 sensors. The film doesn't have the same thickness in all its area, this will make a difference in the initial resistance as will be possible to see in the graphics on the results' chapter. The sensors were numbered as sensor 1 (s1), sensor 2 (s2) and sensor 3 (s3). The montage is shown in Figure 38.

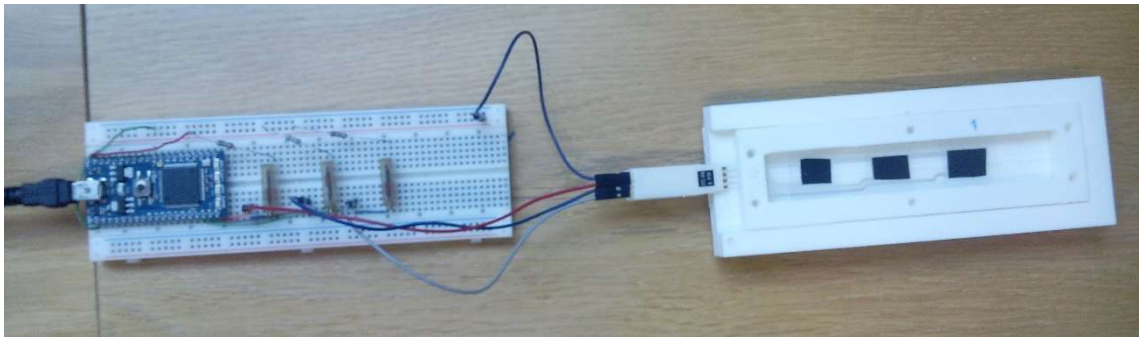

Figure 38. Illustration of all the initial prototype. Sensors are numbered from the left to the right of the sensors platform.

The initial value of each sensor was taken before each test and the value was used to tune the rheostats. This is an important step to get the maximum sensibility of the voltage divider. All the test explained below are organized, for an easier understanding, on Table 1 and Table 2.

Resting Test

After being submitted to random forces, never higher than 10N, the sensors elements were left resting for 2 hours. After this time, they were reconnected to the measurement chain and were left to rest for 50 hours. The goal of this test is to observe the variation of their resistances over the time, when no force is being applied on them.

Temperature Test

The temperature test was made with the help of a domestic heater. The test took 18 hours. In the first two hours, the sensors were submitted to the heater. Then, the heater was turned off but we kept measuring the signal for 16 more hours. For this test, the main objective is to check if the temperature has influence in the transducers resistance and, if it does, analyze if it recovers the initial value when it returns to the room temperature.

Force Test

Before performing the force tests, there are some specifications that need to be understood. First, the force shall be applied in a perpendicular direction. Second, we found that if we put a piece of a softer material between the transducer and the cylinder, like cork, we would obtain a higher resistance variation with the same applied force.

The tests made with discrete forces used the configuration that is shown on Figure 39. The white cylinder has a despicable mass. A rectangle of cork, with the same lengths of the transducer sample, is making the contact between the cylinder and the transducer.

The force tests can be divided in two, the discrete weight test and the continuous test. The first one was made with the metallic weight of 130g and the second one was made with a squeezer *Shimadzu*, Figure 40.

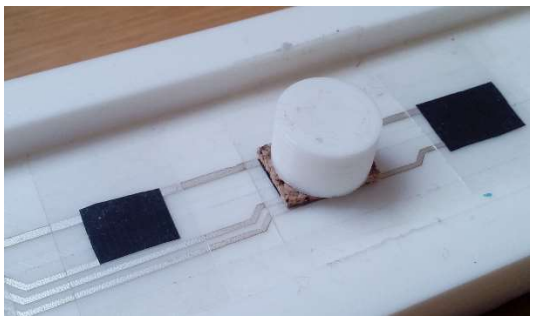

Figure 39. Configuration used to make the force tests.

Figure 40. Squeezer used in the cyclic tests.

Discrete Weight Tests

For each sensor, different cycles were defined. The cycles were designed to test the reaction time, the recovering time and the variation during the increase and decrease of pressure. Other verification that we made with this test is the influence between the different sensors on the array. Cycles are defined in Table 1 and Table 2.

Continuous Cycles Tests

Here, test runs in a different way. The squeezer was programmed to make cycles between a defined pressure and zero during *n* cycles with a frequency *f*. These tests were very important to observe how does the sensor answer to different frequencies and to trace the force/voltage curves. With the results of these tests, the response in frequency was analyzed and the curves of the hysteresis were traced.

5. Results and Discussion

5.1 Resting Tests

This test was made after assembling the transducer with the electrodes. Two hours before the test, the sensors were submitted to stress. In Figure 41, is possible to see the results of 50 hours of test. The result of this test is clear. The transducers keep the same resistance all over the time when they are not submitted to any stress. This means that even the variation of the room temperature between day and night don't have a visible influence in the initial resistance.

Other observation that can be made from this test is the difference between the initial resistance of each transducer. For example, between the sensor 1 and sensor 3 there's a difference of $\pm 16k\Omega$. This shows the need of an adaptation of the measurement bridge when it's shared with many transducers.

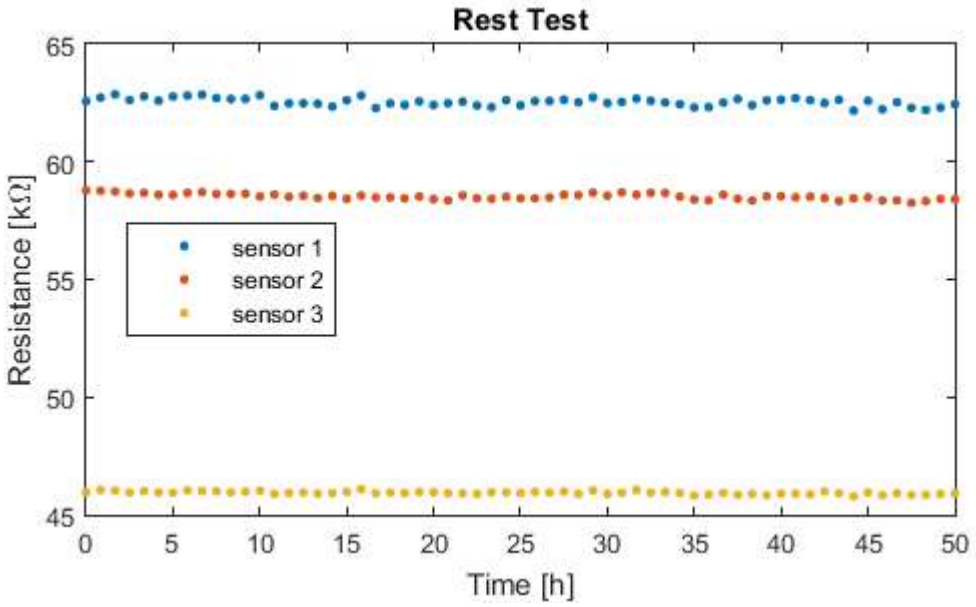

Figure 41. Results of the rest test.

5.2 Temperature Tests

In temperature tests, Figure 42, is important to refer that the temperature variation is not completely controlled. However, it's possible to make a general evaluation of this parameter so we can have an idea of how much can our measurements be affected by this parameter. As is possible to see in the graphic below, the temperature has a small influence in the resistance of the transducers, the resistance tends to increase during the increasing of temperature, $\pm 1\%$. Moreover, the resistance starts to recover to the initial value when the temperature returns to the initial value.

Temperature has some influence. However, for the applications studied in this work, we can consider this influence as minimal.

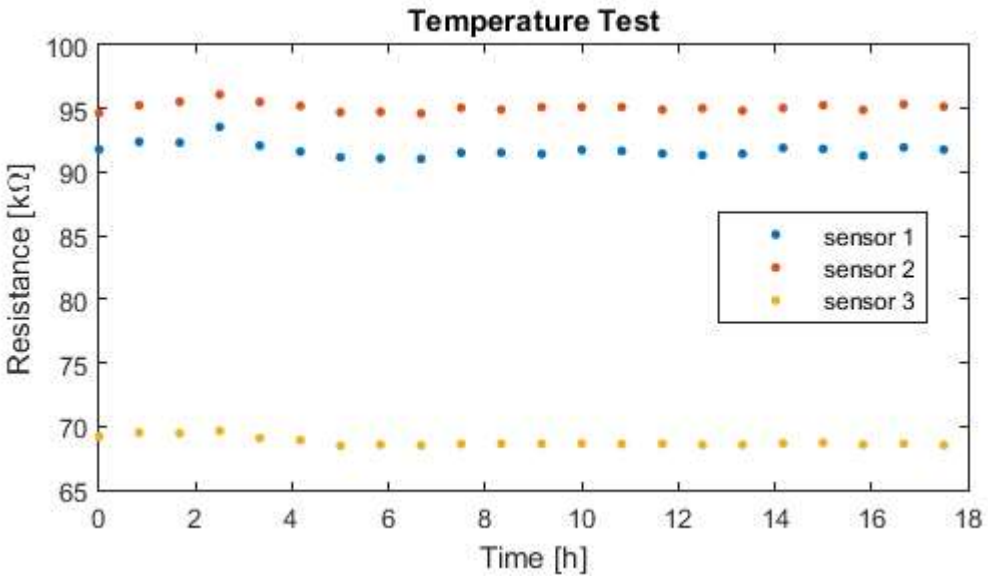

Figure 42. Results of the temperature tests.

5.3 Pressure Tests

5.3.1 Discrete Weight Tests

Discrete tests were made in two different sequences that we call test 1 and test 2. Each one is explained below. The weights were put and took from the transducers manually. This is important to refer because, a manual transference of weights can put artefacts in our signals.

Results Test 1

The weights that were used in each minute of this test are available in the attachments Table 1.

Transducer 1

For transducer's 1 test, Figure 43, we can see that until minute 22 no weight was put over the transducer. On minute 22, three weights are put over and a response is observed. In minute 23, one of the weights is taken, we can see that the resistance goes over the initial value, but quickly comes to an intermediate value (between the initial resistance and the resistance with 3 weights). This shows what we already have concluded before. The way how we take out the weights has a big influence in the response of the transducer. In this case, what probably happened was that we took the weight in a diagonal direction. This led to the support to be inclined, what makes the transducer stays without any weight, for some moments. This creates an overreaction. On minute 25, when all the weights are taken off, it's possible to see that the resistance doesn't reach the initial value. This can be a result of the change in the contacts between the sensing element and the transducer, explained in the subchapter materials and methods.

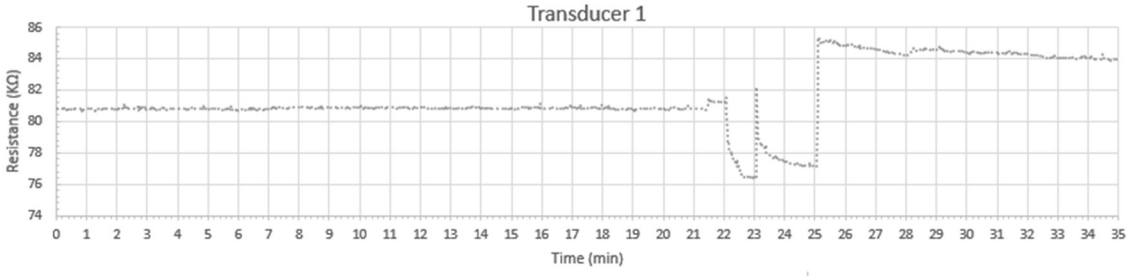

Figure 43. Result of test 1 for transducer 1.

Transducer 2

For transducer's 2 test, Figure 44, there's only one detail that should be added. In minute 2, when one weight is put over the transducer, we almost don't see a response. This shows that there's a limit before the sensor start giving a real response, in this case, the force applied by one weight is not enough to create a variation on the resistance of the sensor.

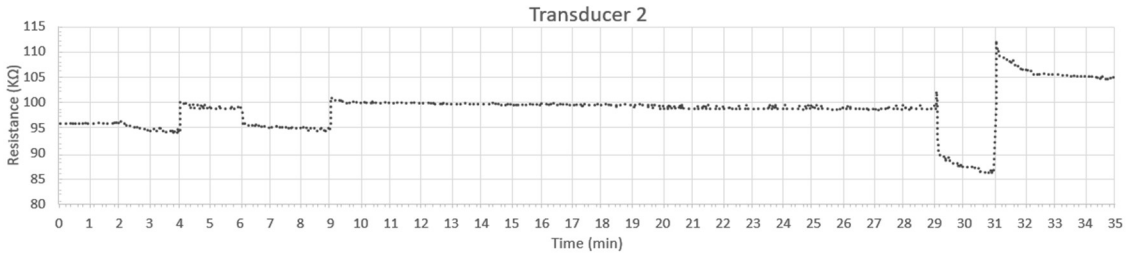

Figure 44. Result of test 1 for transducer 2.

Transducer 3

Transducer's 3 test, Figure 45, shows that the behavior is similar for all the sensors in the array, but doesn't add any extra information.

With test 1 we observed some details as the overshoot and the recuperation. Each time the pressure applied on transducer changes, there's always an overshoot. After other tests, we observed that this overshoot comes from the way we move the weight while placing and removing them.

Another observation we can make from this test's results is that the transducers don't come back to the initial value. Besides this, we cannot take any conclusions at this moment, it's necessary to analyze the test 2 to evaluate this part.

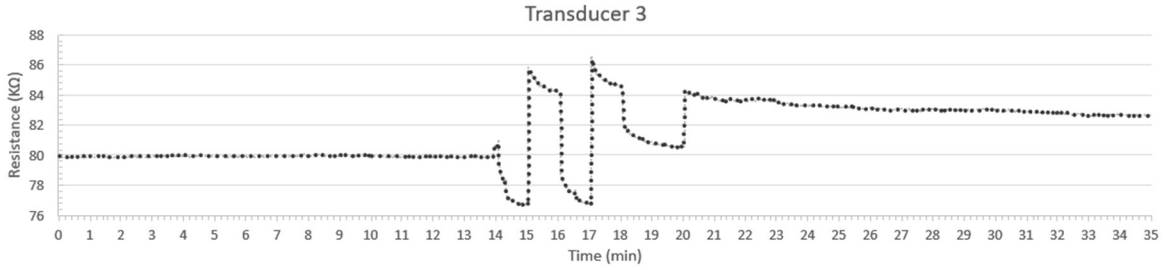

Figure 45. Result of test 1 for transducer 3.

Discussion of Results

The first observation we can make is that every time we withdraw a weight we get an overshoot. The resistance, instead of going through the initial value, increases more than 5% of the initial value, in some cases, then it starts to return to the initial resistance, but takes a long time.

For the graphics of both sensors, we can see that each time we add a weight, the response is exponential, i.e. if a weight is supposed to create a variation of resistance of $5K\Omega$ we observe that around $2K\Omega$ change in less than two seconds, however the other $3K\Omega$ take almost 24 seconds to be reached.

The response of the transducers is fast and clearly visible, however, we must work more on the repeatability. Controlling the resting resistance is also an important step, because, until now, when we remove the weight we don't have a reasonable recover of the initial value.

Finally, we observe in this test that there are no interferences between the transducers.

Results Test 2

The weights that were used in each minute of this test is available in the attachments Table 2.

This test has the same structure of test 1. However, this one is made with more cycles and for a longer time, since test 1 didn't allow us to analyze the behavior for more than two variations of weights. With this test, we expect to understand if after many cycles the behavior becomes repeatable. In Figure 46, Figure 47 and Figure 48 we can observe the results of the response of the three transducers in test 2.

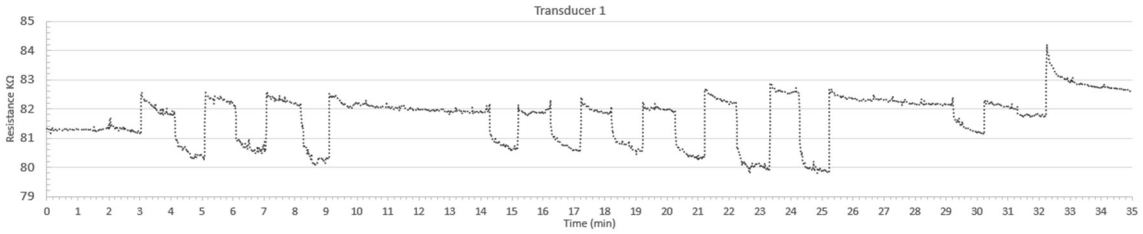

Figure 46. Result of test 2 for transducer 1.

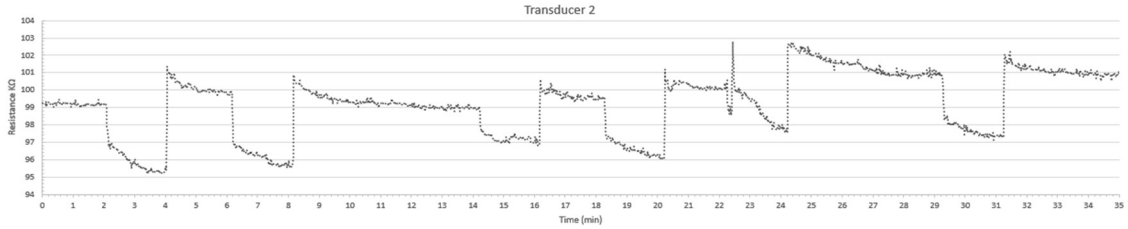

Figure 47. Result of test 2 for transducer 2.

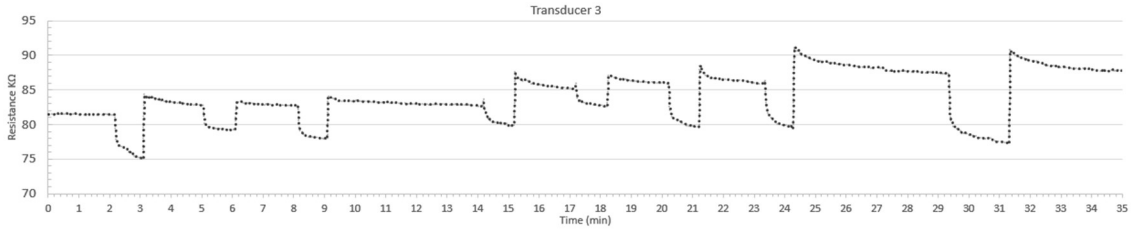

Figure 48. Result of test 2 for transducer 3.

Discussion of Results

To this series of tests there's no need to analyze the transducers one by one. We can see that we got a better repeatability. This is congruent with the information that we have on the paper of the transducer used [4]. For now, we can't evaluate the repeatability of this material. However, with test 2 we observe that it will be possible to manipulate the transducers from the assembly to get better results. Finally, we can conclude that at this point this sensor is not giving good quantitative results. However, we already could use them to make qualitative measurements.

The long recovering time is possible to observe in transducer 2 between the minutes 8 and 14. Other particularity that we can observe is that the curve is not completely synchronized with the table values, this happens not only because of the overshoot, that happens before the response, but also because the user didn't put the weight perfectly synchronized with the time.

Like in test 1, the second test shows us an alteration of the base resistance over the time. We found that this can have origin in three different situations. The first one we already highlight in the beginning of this work, which is the connection between the transducer and the electrodes. The second might be the material itself, that takes a long time to recover to the initial value. Finally, the third situation can be the stress provoked to the transducer, i.e. if we apply a deformation that is bigger than the maximum the material can tolerate, the response can take a longer time to recover and sometimes can't recover at all.

It's not possible, with the test we made, to say that we exceed the deformation value. During the compression, we have other materials being compressed beside the transducer, like the cork.

5.3.2 Continuous Cycles Tests

Continuous tests were made using the squeezer, shown in Figure 40. Here we used the same setting from the discrete tests, Figure 39. The goal in this part is to study the answer of the transducer for different frequencies and to study the hysteresis curve that is common in this kind of materials.

Noncommercial Sensor

With the noncommercial transducers, we have a small variation on the resistance, as we can see in the graphics of the discrete tests. The variation is $\pm 4K\Omega$. Because of this variation, we had to amplify the signal to the maximum range of the ADC. This solution let us see better the hysteresis curve, however, the noise that we get from the squeezer is amplified too.

We started with a test that applies a force in cycles between 0 and 45N, Figure 49. After this test, we made other ones with forces changing between 0 and 25 N because we realized that we got more hysteresis in this range of values, Figure 50. Both tests were made with 0.1Hz (6 cycles/min).

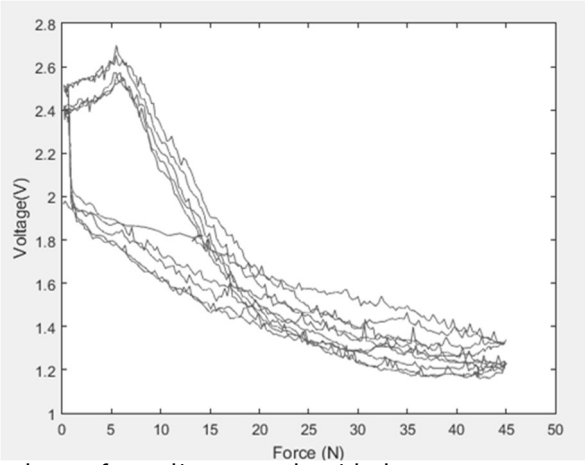

Figure 49. Graphic force/voltage of a cyclic test made with the squeezer.

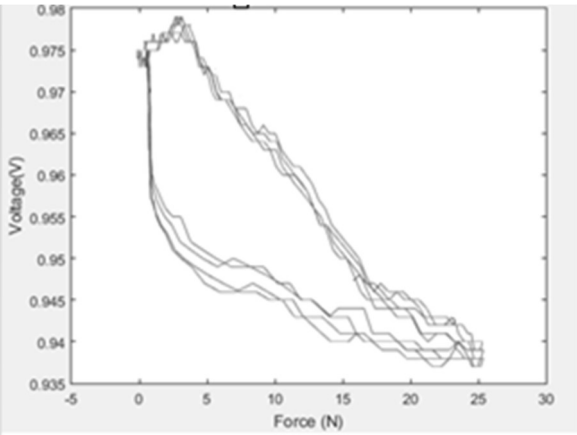

Figure 50. Graphic force/voltage of a cyclic test made only in the hysteresis zone.

Discussion of Figure 49 **and** Figure 50

In relation to the hysteresis, we can see in Figure 49, that the transducer is more hysteretic between 0 and 15 N than for more than 15 N of applied force. Other situation we can observe is that between 0 and 2 N we almost have a vertical response during the release of the pressure, however, after the curve is drawn to the Preisach model, all these situations can be considered.

Other point that can be analyzed with these results is the drift of the responses in each cycle. In Figure 49, we can see that all the curves start being lower after some cycles. This probably happened because of some interference of the assembly. However, if we analyze the first curves separately we can observe that there's a low drift coefficient, at least for that number of cycles. Between each half of the cycles the transducer has a good repeatability.

In Figure 50, we can only see the most hysteretic part of the non-commercial transducer. This is, the curve that can be used to trace the maximum loop used in Preisach model. We can highlight too what was said before about the drift. As it's possible to see, there's almost no drift between a small number of cycles. The drift will be better analyzed in Figure 51 and Figure 52 with a test that was made for 25 cycles.

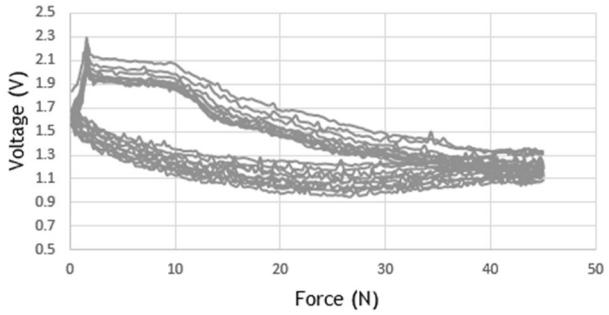

Figure 51. Hysteresis curve of a piezoresistive transducer during the first 12 cycles of tests.

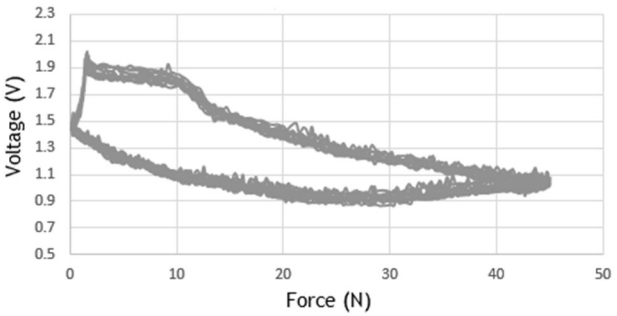

Figure 52. Hysteresis curve of a piezoresistive transducer during the lsat 12 cycles of tests.

Discussion of Figure 51 **and** Figure 52

In the graphic in Figure 51 and Figure 52, we can see the drift of the response between the first and the last cycles. We can also see that the drift after 12 cycles is lower than in the beginning of the experiment. The result expected in a test with more cycles is that the drift will trend to 0 after 100 cycles, as described in [4].

The repeatability is a characteristic of this material. Although we always have hysteresis, the characteristic curve behaves every time in the same way. At this point of the work is possible to say that for one transducer, we have repeatability and a low drift coefficient. However, the assemblage method must be improved because that's the only way to reduce the number of variables of the system.

Commercial Transducer

The commercial transducer has one big difference in relation of the noncommercial transducer. Its resistance varies from $+\infty$ to $1k\Omega$. When no force is being applied, the transducer is not in

contact with the electrodes, this happens because of the assembling mode. If we see the Figure 53, after two or three newtons of applied force, the transducer enters in contact with the electrodes and the differential voltage starts decreasing. We can see that when the force is near to zero we have a saturated response $\pm 3.3V$. It's possible to observe too that after the second cycle we have a very slow drift between 2 and 4%, that is less than 5% as the specifications of the product [27].

The curve was traced with a cyclic force that goes from 0 to 30 N, each cycle. This was the lowest frequency tested. However, higher frequencies were tested too. Figure 54 shows an example of what happen when we try to change the frequency of the applied cycles. We can see that the hysteresis is so high that we can't even consider making an approach using the Preisach model.

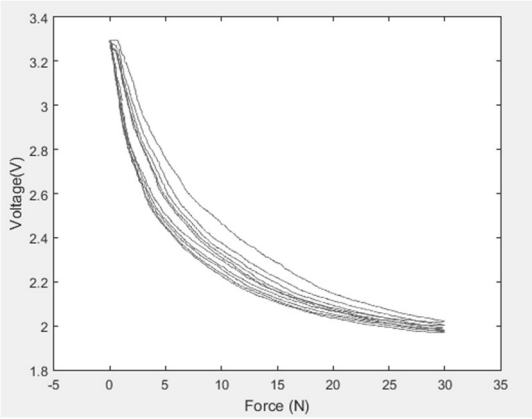

Figure 53. Hysteresis curve of the commercial PS used in this project.

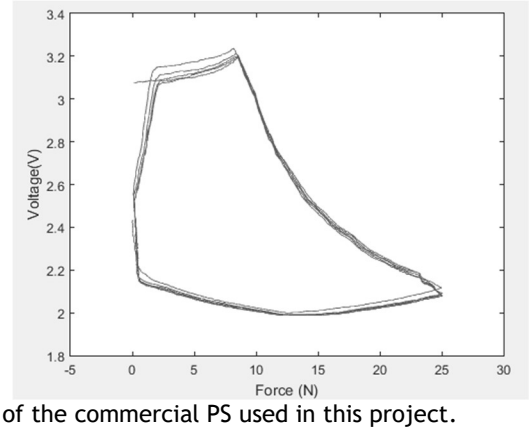

Figure 54. Hysteresis curve of the commercial PS used in this project.

Discussion of Figures 51 e 52

In Figure 53 we can see a good response with almost no drift. Only the first cycle has more drift but, that's only the adjustment of the squeezer. This transducer doesn't have a linear response and besides that, it shows a hysteretic behavior. This could be a problem if we were expecting to make a simple linearization before using this transducer. However, that's a good opportunity

to put in practice the Preisach model. This is the curve that will be used to test the Preisach model in this project.

The graphic from Figure 54 is presented to illustrate the dependence of the speed for this kind of transducer. We can see that the frequency in this case makes all the difference.

For the continuous tests, we can observe that both transducers have hysteresis and a similar drift coefficient. Other interesting point is that, for higher frequencies, the transducers present lower hysteresis.

With this we can verify the following points about the non-commercial transducer in relation to the commercial transducer:

- Smaller resistance variation;
- Longer recuperation time;
- Better response for high frequencies;
- Higher hysteresis area.

There are other characteristics that can look obvious at this point, for example, the commercial transducer shows a higher repeatability. However, we can't take this conclusion at this moment because there are factors, as the assembly method of the transducers, that are yet to be reviewed.

6. Conclusions and Future Work

Although this is not a pioneer work in this field, even for our laboratory, it brought a new perspective in relation to PSs. Today, because we can produce the sensors by screen printing technologies using green chemicals, it's possible to spread the areas of application of this kind of sensors.

The biggest obstacle of PSs with a wide deformation capacity is their precision. Although the measuring of high deformations doesn't require high precision, sometimes we can ask for more precisely measurements. This is a problem with PSs. They have hysteresis, drift and a nonlinear response. To overcome this situation, we started to adapt the Preisach model that can make a better approach to systems with hysteresis. The model was adapted successfully and inputs in offline mode were given to the system. We saw that this approach is possible.

Now it's necessary to give a step forward with the Preisach model. After we get the maximum loop function we can use it to let the system receive online voltage values calculating with this the force that is being applied.

The choice of the materials used as transducers for this work was directly related with the partnership that we have with the Electroactive Smart Materials laboratory from University of Minho. They supplied us with their transducers when we needed them. We used commercial transducers too. They were important to make a comparison of results. The commercial sensor and the components to the electronic circuit were chosen by the parameters we needed and by their availability.

With concern to this work, we could say that the objectives set were accomplished. We produced three versions of a data acquisition system. We developed and assembled our own transducer and then we tested it with the data acquisition system. We did all the steps behind the production of a wireless smart sensor.

In the end of this work, we don't have a product that can be put on the market. The reason is that some of the techniques must be improved, because we didn't get good enough results to make this a commercial product. For example, the assemblage method must be improved and stabilized, because the way we did it doesn't guarantee that we will always have the same result.

With concern to the transducer used we can say that the material has potential and is a good solution for high deformation measurements. However, a plastic conductor must be developed to avoid the problem with broken pads. In fact, our partners are already working in this situation. One interesting point of the non-commercial sensors is their adaptability. With the existent technologies, we can create them as flexible and conductor as we want.

The PCB works as it supposed, but some improvements can be done. For instance, the MCU and the wifi module can be changed by other components that can do the same work but that are cheaper than the ones we used in the prototype. Another thing that can be done is the reduction of the dimension of the third prototype.

The software in general doesn't have big changes to do. However, the graphic user interface (GUI) should be completely redefined if we want to make it user friendly for common users. The Preisach model must be adapted to work online. In this project, the design of the user interface was not a priority since we needed the results first. Finally, and still coming back to the Preisach model, we can say that it has good odds to work, however, we only made the mathematical application. This means that, to ensure that this model can be applied with these sensors, we first need to make practical tests with it.

Some more studies in this field can be considered in future works, for example, we didn't consider the influence of the temperature in the variation of the resistance. We saw that the transducers' resistance didn't change too much during the temperature variation, but we didn't check if the temperature changes the deformation properties of the material.

This work required knowledge in the most diversified areas, from chemistry to physics, electronics, programming and mathematics. It was a great opportunity to deep in the world of instrumentation. In fact, more than the final product of this work, a knowledge pool was acquired.

7. Bibliography

[1] K. Kalantar-zadeh and B. Fry, “Sensor Characteristics and Physical,” in *Nanotechnology-Enabled Sensors*, 1st ed., Springer, Ed. Springer US, 2008, pp. 13–30.

[2] C. S. Smith, “Piezoresistance Effect in Germanium and Silicon,” *Phys. Rev.*, vol. 94, no. 1, pp. 42–49, 1954.

[3] H. P. Wong, S. Mitra, D. Akinwande, C. Beasley, Y. Chai, H. Chen, X. Chen, G. Close, J. Deng, A. Hazeghi, J. Liang, A. Lin, L. S. Liyanage, J. Luo, J. Parker, N. Patil, M. Shulaker, H. Wei, L. Wei, and J. Zhang, “Carbon Nanotube Electronics – Materials , Devices , Circuits , Design , Modeling , and Performance Projection,” vol. 1, pp. 501–504, 2011.

[4] B. F. Gonçalves, P. Costa, J. Oliveira, S. Ribeiro, V. Correia, G. Botelho, and S. Lanceros-Mendez, “Green solvent approach for printable large deformation thermoplastic elastomer based piezoresistive sensors and their suitability for biomedical applications,” *J. Polym. Sci. Part B Polym. Phys.*, vol. 54, no. 20, pp. 2092–2103, 2016.

[5] J. J. Wang, C. E. Lu, J. L. Huang, R. Chen, and W. Fang, “Nanocomposite rubber elastomer with piezoresistive detection for flexible tactile sense application,” *Proc. IEEE Int. Conf. Micro Electro Mech. Syst.*, vol. 2, pp. 720–723, 2017.

[6] S. Luo and T. Liu, “Structure-property-processing relationships of single-wall carbon nanotube thin film piezoresistive sensors,” *Carbon N. Y.*, vol. 59, pp. 315–324, 2013.

[7] “GLOBAL.” [Online]. Available: http://www.globalindustrial.com/p/packaging/bags/on-rolls/black-conductive-tubing-4-4-mil-750-rl?utm_source=shopping&utm_medium=shp&utm_campaign=On-Rolls-shop&infoParam.campaignId=WP. [Accessed: 11-Apr-2017].

[8] “FlexiForce.” [Online]. Available: http://www.flexiforce.com. [Accessed: 10-Mar-2017].

[9] H. Deng, L. Lin, M. Ji, S. Zhang, M. Yang, and Q. Fu, “Progress on the morphological control of conductive network in conductive polymer composites and the use as electroactive multifunctional materials,” *Prog. Polym. Sci.*, vol. 39, no. 4, pp. 627–655, 2014.

[10] I. I. Nefedova, D. V. Lioubtchenko, and A. V. Raisanen, “Conductivity of Carbon Nanotube Layers at Low-Terahertz Frequencies,” *IEEE Trans. Terahertz Sci. Technol.*, vol. 6, no. 6, pp. 840–845, 2016.

[11] G. Maitre, D. Gabioud, and P. Roduit, “Local algorithm for the open loop control of thermostatically controlled loads,” *IEEE PES Innov. Smart Grid Technol. Conf. Eur.*, vol. Part F1264, 2017.

[12] W. Kim, A. Javey, O. Vermesh, Q. Wang, Y. Li, and H. Dai, “Hysteresis caused by water molecules in carbon nanotube field-effect transistors,” *Nano Lett.*, vol. 3, no. 2, pp. 193–198, 2003.

[13] J. J. TYSON and B. NOVAK, “Regulation of the Eukaryotic Cell Cycle: Molecular Antagonism, Hysteresis, and Irreversible Transitions,” *J. Theor. Biol.*, vol. 210, no. 2, pp. 249–263, 2001.

[14] R. Cross, “On the Foundations of Hysteresis in Economic Systems,” *Econ. Philos.*, vol. 9, no. 1, p. 53, 1993.

[15] Augusto Visintin, *Models of Hysteresys*. Longman Scientific & Technical, 1993.

[16] Augusto Visintin, *Differential Models of hysteresis*. Springer, 1994.

[17] P. M. Sain, M. K. Sain, and B. F. Spencer, “Models for hysteresis and application to structural control,” *Proc. 1997 Am. Control Conf. (Cat. No.97CH36041)*, vol. 1, no. June, pp. 16–20, 1997.

[18] I. Mayergoyz, *Mathematical Models of Hysteresis and their Applications*. Maryland: Elsevier, 2003.

[19] J. Park and S. Mackay, “Practical Data Acquisition for Instrumentation and Control Systems,” p. 435, 2003.

[20] T. Instruments, “INA333 DataSheet.” Texas Insruments, 2015.

[21] “MAX5391 / MAX5393 Dual 256-Tap DataSheet.” maxim integrated, 2014.

[22] Vishay, “Vishay Siliconix Precision 8-Ch / Dual 4-Ch / Triple 2-Ch Low Voltage Analog Switches / Multiplexers.” 2011.

[23] V. Jani, V. Ili, N. Pjevalica, and M. Niko, “An approach to modeling the hysteresis in ferromagnetic by adaptation of Preisach model,” *22nd Telecommun. forum TELFOR 2014*, pp. 761–764, 2014.

[24] “Mbed Website.” [Online]. Available: https://developer.mbed.org/platforms/mbed-LPC1768/.

[25] I. Roving Networks, “RN-171-XV 802 . 11 b / g Wireless LAN Module DataSheet.” 2012.

[26] Microchip Technology Inc., “WiFly Command Reference, Advanced Features and Applications User’s Guide.” pp. 1–122, 2014.

[27] F. S. R. Series, R. Force, and S. Resistor, “FSR 400 Data Sheet Interlink Electronics - Sensor Technologies,” pp. 1–4.

8. Attachments

Table 1. Table of test 1 with discrete weight.

	Mass applied in each transducer (g)		
Time (min)	Transducer 1	Transducer 2	Transducer 3
0	0	0	0
1	0	0	0
2	0	130	0
3	0	130	0
4	0	0	0
5	0	0	0
6	0	260	0
7	0	260	0
8	0	260	0
9 a 13	0	0	0
14	0	0	130
15	0	0	0
16	0	0	130
17	0	0	0
18	0	0	130
19	0	0	130
20	0	0	0
21	0	0	0
22	390	0	0
23	260	0	0
24	260	0	0
25 a 28	0	0	0
29	0	260	0
30	0	260	0
31 a 34	0	0	0

Table 2. Table of test 2 with discrete weight.

	Mass applied in each transducer (g)		
Time (min)	Transducer 1	Transducer 2	Transducer 3
0	0	0	0
1	0	0	0
2	130	130	260
3	0	130	0
4	130	0	0
5	0	0	260
6	130	130	0
7	0	130	0
8*	130	0	260
9 a 13	0	0	0
14	130	130	260
15	0	130	0
16	130	0	0
17	0	0	260
18	130	130	0
19	0	130	0
20	130	0	260
21	0	0	0
22*	130	130	0
23	0	130	260
24	130	0	0
25 a 28	0	0	0
29	130	130	260
30	0	130	260
31	130	0	0
32 a 130	0	0	0
148	0	0	130
149	0	0	260
150	0	0	390
151	0	0	520
152	130	0	390
153	260	0	260
154	390	0	130
155	0	0	0
156	0	0	0
157	0	0	0
158	0	0	0
159	0	0	0
160 a 400	0	0	0
115 a 400	0	0	0

*Here a perturbation happened, is possible to observe it in the correspondent graphic.